Monthly Notices
of the
ROYAL ASTRONOMICAL SOCIETY

MNRAS **470,** 800–814 (2017)
Advance Access publication 2017 May 9

doi:10.1093/mnras/stx1117

BAT AGN Spectroscopic Survey (BASS) – VI. The Γ_X–L/L_{Edd} relation

Benny Trakhtenbrot,[1★†] Claudio Ricci,[2,3] Michael J. Koss,[1,4‡] Kevin Schawinski,[1] Richard Mushotzky,[5] Yoshihiro Ueda,[6] Sylvain Veilleux,[5] Isabella Lamperti,[1,7] Kyuseok Oh,[1] Ezequiel Treister,[2] Daniel Stern,[8] Fiona Harrison,[9] Mislav Baloković[9] and Neil Gehrels[10§]

[1]*Institute for Astronomy, Department of Physics, ETH Zurich, Wolfgang-Pauli-Strasse 27, CH-8093 Zurich, Switzerland*
[2]*Instituto de Astrofísica, Facultad de Física, Pontificia Universidad Católica de Chile, Casilla 306, Santiago 22, Chile*
[3]*Kavli Institute for Astronomy and Astrophysics, Peking University, Beijing 100871, China*
[4]*Eureka Scientific Inc., 2452 Delmer St. Suite 100, Oakland, CA 94602, USA*
[5]*Department of Astronomy and Joint Space-Science Institute, University of Maryland, College Park, MD 20742, USA*
[6]*Department of Astronomy, Kyoto University, Kyoto 606-8502, Japan*
[7]*Astrophysics Group, Department of Physics and Astronomy, University College London, 132 Hampstead Road, London NW1 2PS, UK*
[8]*Jet Propulsion Laboratory, California Institute of Technology, 4800 Oak Grove Drive, MS 169-224, Pasadena, CA 91109, USA*
[9]*Cahill Center for Astronomy and Astrophysics, California Institute of Technology, Pasadena, CA 91125, USA*
[10]*NASA Goddard Space Flight Center, Greenbelt, MD 20771, USA*

Accepted 2017 May 5. Received 2017 May 4; in original form 2017 March 27

ABSTRACT

We study the relation between accretion rate (in terms of L/L_{Edd}) and shape of the hard X-ray spectral energy distribution (namely the photon index Γ_x) for a large sample of 228 hard X-ray-selected, low-redshift active galactic nuclei (AGNs), drawn from the *Swift*/BAT AGN Spectroscopic Survey (BASS). This includes 30 AGNs for which black hole mass (and therefore L/L_{Edd}) is measured directly through masers, spatially resolved gas or stellar dynamics, or reverberation mapping. The high-quality and broad energy coverage of the data provided through BASS allow us to examine several alternative determinations of both Γ_x and L/L_{Edd}. For the BASS sample as a whole, we find a statistically significant, albeit very weak correlation between Γ_x and L/L_{Edd}. The best-fitting relations we find, $\Gamma_x \simeq 0.15 \log L/L_{Edd} + \text{const.}$, are considerably shallower than those reported in previous studies. Moreover, we find *no* corresponding correlations among the subsets of AGN with different M_{BH} determination methodology. In particular, we find no robust evidence for a correlation when considering only those AGN with direct or single-epoch M_{BH} estimates. This latter finding is in contrast to several previous studies which focused on $z > 0.5$ broad-line AGN. We discuss this tension and conclude that it can be partially accounted for if one adopts a simplified, power-law X-ray spectral model, combined with L/L_{Edd} estimates that are based on the continuum emission and on single-epoch broad-line spectroscopy in the *optical* regime. We finally highlight the limitations on using Γ_x as a probe of supermassive black hole evolution in deep extragalactic X-ray surveys.

Key words: black hole physics – galaxies: active – quasars: general – X-rays: galaxies.

1 INTRODUCTION

One of the major goals in the study of active galactic nuclei (AGN) is to understand how basic physical properties of the accreting supermassive black hole (SMBH) are linked to the emergent (continuum) radiation field. The ultraviolet (UV)-optical continuum can be explained by (thin) accretion discs, in a way which involves the BH mass (M_{BH}), accretion rate (in terms of the Eddington ratio, L/L_{Edd}), and the BH spin, through deterministic, analytical and/or numerical models (e.g. Davis & Hubeny 2006; Done et al. 2012; Netzer 2013, and references therein). This is not the case with the X-ray continuum emission, which is thought to originate from a compact, hot corona that surrounds the inner parts of the accretion disc and Compton upscatters the disc UV photons. Indeed, it is not yet clear

★ E-mail: benny.trakhtenbrot@phys.ethz.ch
† Zwicky Fellow.
‡ Ambizione Fellow.
§ Deceased 2017 February 6. This work is dedicated to his memory.

whether this significant emission component can be directly linked to any key AGN properties, from both theoretical and observational perspectives.

In the energy range ∼0.5–10 keV, the intrinsic X-ray continuum emission is observed to follow a power law of the form $dN/dE \propto E^{-\Gamma_x}$. Early evidence for a correlation between Γ_x and L/L_{Edd} was put forward by several studies that focused mainly on specific high-Γ_x AGN and/or on narrow-line Seyfert 1 sources (e.g. Pounds, Done & Osborne 1995; Brandt, Mathur & Elvis 1997; Brandt & Boller 1998; Porquet et al. 2004; Wang, Watarai & Mineshige 2004; Bian 2005). These sources, which are generally thought to represent the high-L/L_{Edd} end of the (local) AGN population, exhibit soft X-ray spectra (i.e. high Γ_x). However, the limited size and range of luminosities probed in these early studies prohibited them from ruling out a scenario where the fundamental underlying relation is driven by L_{AGN} (or M_{BH}), rather than L/L_{Edd}.

Since then, several studies have provided an increasingly more complete picture of this proposed relation by probing AGN that cover a wide range of luminosities and redshifts. These include the studies of Shemmer et al. (2006) and Shemmer et al. (2008, hereafter S08), which were the first to provide measurements for a substantial sample of $z > 3$, extremely luminous quasars; Risaliti, Young & Elvis (2009, hereafter R09), which relied on a large sample of quasars drawn from the Sloan Digital Sky Survey (SDSS), at $0 \lesssim z \lesssim 4.5$; Brightman et al. (2013, hereafter B13), which used dozens of unobscured, moderate-luminosity AGN at $0.5 \lesssim z \lesssim 2$, from the COSMOS survey; and Fanali et al. (2013), which studied a sample of unobscured AGN from the *XMM-Newton* Bright Serendipitous Survey. The common result of these studies is the identification of a robust, statistically significant positive correlation between Γ_x, usually measured over the observed-frame range of ∼2–10 keV, and L/L_{Edd}. Moreover, these studies demonstrated that L/L_{Edd} is indeed the main driver of this relation, and not L_{AGN} and/or M_{BH}. Most recently, the study of Brightman et al. (2016) showed that the Γ_x–L/L_{Edd} relation is also applicable to local Compton-thick (CT) AGN, using a small sample of sources for which precise, maser-based determinations of M_{BH} are available. Finally, several X-ray variability studies identified a trend of increasing Γ_x with increasing flux levels for individual systems (e.g. Magdziarz et al. 1998; Zdziarski et al. 2003; Sobolewska & Papadakis 2009), which may be interpreted as the consequence of a strong, positive correlation between L/L_{Edd} and Γ_x for any given accreting BH.

Besides the implications for small-scale physics of the X-ray emitting coronae near accreting SMBHs, S08 and the studies that followed highlighted the prospect of using Γ_x, measured in deep X-ray surveys extending to $z \sim 5$ (e.g. Brandt & Alexander 2015), to study the distribution of L/L_{Edd} and hence of M_{BH} (assuming a bolometric correction), in virtually *all* classes of AGN, including obscured sources where L/L_{Edd} and M_{BH} are otherwise unavailable. Moreover, it has been shown that a positive relation between Γ_x and L/L_{Edd} would be able to explain the X-ray Baldwin effect (Ricci et al. 2013), i.e. the decrease of the Fe Kα equivalent width with increasing luminosity and L/L_{Edd} (e.g. Iwasawa & Taniguchi 1993; Bianchi et al. 2007).

A possible explanation of the Γ_x–L/L_{Edd} relation is that for high L/L_{Edd} the intense UV/optical radiation, which provides the seed photons for the X-ray emission, can lead to a more efficient cooling of the X-ray corona, decreasing the temperature, and/or optical depth of the plasma. Lower temperatures and/or optical depths of the corona, in turn, would then result in a softer X-ray spectral energy distribution (SED; i.e. higher Γ_x). This would also be in agreement with the positive correlation between L/L_{Edd} and the ratio of the UV/optical-to-X-ray flux found in several studies (see e.g. S08; Grupe et al. 2010; Lusso et al. 2010; Jin, Ward & Done 2012, but also Vasudevan & Fabian 2007; Vasudevan et al. 2009). Another explanation involves the growth of instabilities in a two-phase, disc-corona accretion flow, which would also explain the flattening (or, indeed, reversal; see below) of the Γ_x–L/L_{Edd} relation at low accretion rates (Yang et al. 2015; Kawamuro et al. 2016b).

It is worth bearing in mind, however, that virtually all the studies that reported Γ_x–L/L_{Edd} correlations used a relatively limited X-ray energy range, dictated by the capabilities of the *Chandra* and *XMM-Newton* facilities (i.e. ∼0.5–10 keV). One may suspect that this limited energy range may not be broad enough to account for the rich collection of phenomenological and physical radiation components which constitute the X-ray SED of AGN. In particular, some studies noted the issues involving the soft excess, the Compton 'hump', and/or the high-energy cut-off, and how the inability to observe these directly may affect the spectral decomposition of the AGN samples under study. Other limitations of the reported positive Γ_x–L/L_{Edd} correlation include the significant amount of scatter observed in the Γ_x–L/L_{Edd} plane, where Γ_x may cover the range $\Gamma_x \sim 1$–2.5 even for a narrow range in L/L_{Edd} ($\lesssim$0.5 dex; see e.g. Ho & Kim 2016). Finally, some studies have claimed that, for slowly accreting and/or low-mass SMBHs, the Γ_x–L/L_{Edd} relation may actually change to become an *anticorrelation* (e.g. Constantin et al. 2009; Younes et al. 2011; Gültekin et al. 2012; Kamizasa, Terashima & Awaki 2012; Yang et al. 2015; Kawamuro et al. 2016b).

A promising way for addressing some of these limitations, and for expanding the Γ_x–L/L_{Edd} relation towards more complete, larger samples of AGN, is to study hard X-ray-selected AGN, for which the spectral coverage in the X-rays extends to higher energies. Indeed, several studies tried to identify relations between Γ_x and L/L_{Edd} in samples of AGN detected by the hard X-ray *Swift*/BAT instrument (covering roughly 15–150 keV; Gehrels et al. 2004), which are essentially free of any obscuration-related selection biases. Some of these earlier *Swift*/BAT studies demonstrated the significant scatter in the Γ_x–L/L_{Edd} plane, and found no convincing evidence for a correlation between these properties – interpreted as a result of the limited sample size (e.g. Winter et al. 2009a,b). The increasing size of *Swift*/BAT-detected AGN samples, combined with more elaborate X-ray spectral analyses, eventually allowed the identification of significant Γ_x–L/L_{Edd} correlations (Winter et al. 2012; Kawamuro et al. 2016a; note that in the former study the correlations are found only when binning the sample by L/L_{Edd}, similarly to B13).

In this study, we seek to establish a relation between Γ_x and L/L_{Edd} for a large and essentially complete sample of low-redshift, hard X-ray-selected AGN. Our sample is based on the first data release of the BAT AGN Spectroscopic Survey (BASS). BASS provides a rich collection of X-ray and optical data for about 642 AGN, mostly at $z < 0.5$, with unprecedented levels of completeness in terms of optical spectroscopy. Compared to other low-redshift AGN samples, the hard X-ray selection that forms the basis of BASS ensures that the resulting sample is minimally affected by the AGN hosts, particularly by obscuring dust and/or contaminating optical line emission. The BASS sample covers a wide range in L_{AGN}, M_{BH}, and L/L_{Edd}, for AGN of essentially all emission line and/or obscuration-based classification. It therefore serves as an ideal benchmark for addressing many open questions concerning the X-ray and optical emission mechanisms in AGN, and how these are related to basic BH properties (Berney et al. 2015; Lamperti et al. 2017; Oh et al. 2017).

This paper is organized as follows. In Section 2, we present our sample and the data from which we measure $L/L_{\rm Edd}$ and $\Gamma_{\rm x}$. In Section 3, we examine possible correlations between these quantities, but conclude that robust and/or strong correlations of this sort cannot be clearly established for our BASS sample of AGN. In Section 4, we discuss our main findings, in the context of the several previous studies that reported $\Gamma_{\rm x}$–$L/L_{\rm Edd}$ relations. Section 5 summarizes our findings. Throughout this work we assume a cosmological model with $\Omega_\Lambda = 0.7$, $\Omega_{\rm M} = 0.3$, and $H_0 = 70\,{\rm km\,s^{-1}\,Mpc^{-1}}$.

2 SAMPLE AND DATA

2.1 The BASS dr1 sample of AGN

This work focuses on AGN selected through their hard-band X-ray emission, as identified in the *Swift*/BAT 70-month catalogue (Baumgartner et al. 2013). Out of 1210 unique objects in that catalogue, 836 have been identified as known AGN. The first data release of the BASS project (Koss et al., in preparation; hereafter K17) includes 642 of these AGN, for which redshifts and complementary multiwavelength data are available. As part of the BASS effort, we have curated optical spectra for 580 AGN, which were then used to measure accurate redshifts and other spectral properties, relying on narrow emission lines (usually [O III] λ5007; see K17). For 62 additional AGN, redshifts are available from the NASA Extragalactic Database (NED).

Of the initial sample of 642 sources with redshifts, we first focus on the 425 AGN for which determinations of $M_{\rm BH}$ are available within BASS. More information regarding these determinations of $M_{\rm BH}$ is provided in Section 2.3 below. We further focus on sources within the redshift range $0.01 < z < 0.5$, thus omitting 40 AGN and leaving in 385 BASS sources. This is done to avoid high-z beamed AGN (and blazars), and also extremely nearby AGN for which the precise distances (and therefore luminosities) may be somewhat uncertain. We finally select only those sources for which the available X-ray observations have a sufficiently high number of counts, i.e. $N_{\rm counts} > 1000$, to ensure a high-quality spectral fit (more information regarding our X-ray data is given in Section 2.2 below).

Our final primary sample therefore consists of 228 AGN at $0.01 < z < 0.5$, which have a high-quality X-ray spectrum and a reliable BH mass determination. These include 30 AGN with 'direct' mass measurements (either from masers, gas or stellar dynamics, or reverberation mapping); 149 AGN with $M_{\rm BH}$ estimates obtained through single-epoch spectra of broad Balmer lines; and 49 AGN for which $M_{\rm BH}$ is determined by combining stellar velocity dispersion (σ_*) measurements and the $M_{\rm BH}$–σ_* relation. We note that – unlike other samples that investigated the relation between $\Gamma_{\rm x}$ and $L/L_{\rm Edd}$ – our final sample consists of both broad- and narrow-line AGN (174 and 54 AGN, respectively).

2.2 X-ray data and analysis

The analysis of the available X-ray data for the BASS AGN was presented in detail in Ricci et al. (submitted; hereafter R17). This analysis included all the X-ray data available for the BASS sample, including *Swift*/XRT, *XMM-Newton*/EPIC, *Chandra*/ACIS, *Suzaku*/XIS, or *ASCA*/GIS/SIS observations, and typically covering the observed-frame energy range of 0.3–150 keV. The X-ray data were fitted with a set of models that rely on an absorbed power-law X-ray SED with a high-energy cut-off, and a reflection component. A cross-calibration constant was applied to each source, in order to account for possible flux variability between the 70-month integrated *Swift*/BAT spectrum and the significantly shorter 0.3–10 keV observations. Additional components accounting for warm absorbers, soft excess, Fe Kα lines, and/or other spectral features were added if deemed necessary to obtain a satisfactory fit to the data. The reader is referred to R17 for a detailed discussion of the models' physical components, parameters, and fitting quality. We note here that the R17 analysis did *not* explicitly impose a finite range of possible $\Gamma_{\rm x}$.

The analysis of the X-ray data provided several ways of determining $\Gamma_{\rm x}$, which we use throughout this study:

(i) First, $\Gamma_{\rm tot}$ denotes the photon index recovered from the entire (relevant) energy range and the full multicomponent model adopted for each source (in which $E_{\rm C}$ is a free parameter). This is the fiducial photon index adopted in the R17 study and throughout the present work (unless otherwise noted).

(ii) $\Gamma_{\rm nEc}$ results from modelling the entire X-ray spectral range with a model which ignores the high-energy cut-off (i.e. setting $E_{\rm C} = 500\,{\rm keV}$).

(iii) $\Gamma_{0.3-10}$ denotes the photon index that describes only the observed-frame 0.3–10 keV energy range, using a model that ignores the high-energy cut-off (which was fixed to $E_{\rm C} = 500\,{\rm keV}$) and the reflection component.

(iv) $\Gamma_{\rm BAT}$ results from fitting a power-law model solely to the energy range probed by *Swift*/BAT (i.e. 14–195 keV).

Fig. 1 presents some of the statistical properties of $\Gamma_{\rm tot}$ for our sources. The left-hand and centre panels show $\Gamma_{\rm tot}$ and the related uncertainty ($\Delta\Gamma_{\rm tot}$), plotted against the number of counts across the available X-ray spectral range, $N_{\rm counts}$. As noted above, in this work we include only BASS AGN with $N_{\rm counts} > 1000$, where the typical uncertainty on $\Gamma_{\rm tot}$ is $\Delta\Gamma_{\rm tot} \lesssim 0.2$. This choice, which we can make only thanks to the high-quality X-ray data in BASS, can be considered conservative – indeed, previous studies of the $\Gamma_{\rm x}$–$L/L_{\rm Edd}$ relation relied on X-ray spectra with significantly fewer counts.[1] The left-hand panel of Fig. 1 suggests that our cut on $N_{\rm counts}$ does not bias our sample against any particular range in $\Gamma_{\rm tot}$.

Our primary sample of 228 AGN with $N_{\rm counts} > 1000$ and $0.01 < z < 0.5$ covers a wide range in $\Gamma_{\rm tot}$ with $\Gamma_{\rm tot} \sim 1$–2.8, a median (and mean) value of $\langle\Gamma_{\rm tot}\rangle = 1.8$, and a standard deviation of $\sigma(\Gamma_{\rm tot}) = 0.27$.

The R17 analysis of the X-ray data for our sources also provides a more detailed and complete method for quantifying the obscuration towards the BASS AGN, based on the (Hydrogen) column density $N_{\rm H}$. Setting the threshold at $\log(N_{\rm H}/{\rm cm^{-2}}) = 22$ splits our primary sample to 162 unobscured and 66 obscured AGN (i.e. with $\log[N_{\rm H}/{\rm cm^{-2}}]$ below and above 22, respectively, and still obeying the redshift and $N_{\rm counts}$ cuts described above). 27 of the AGN in our primary sample are heavily obscured, with $\log(N_{\rm H}/{\rm cm^{-2}}) \geq 23.5$, and 8 of these are CT ($\log(N_{\rm H}/{\rm cm^{-2}}) \geq 24$; see also Ricci et al. 2015).

2.3 Black hole masses, bolometric luminosities and $L/L_{\rm Edd}$

The BH masses available for all our 228 BASS sources were determined through several different methods. First, for 30 sources, we relied on directly measured $M_{\rm BH}$ – either from masers; spatially resolved gas or stellar dynamics; or from reverberation mapping.

[1] For example, only about ∼1/3 of those studied by B13 had $N_{\rm counts} \gtrsim 1000$ (a cut of $N_{\rm counts} > 250$ was applied for the entire B13 sample).

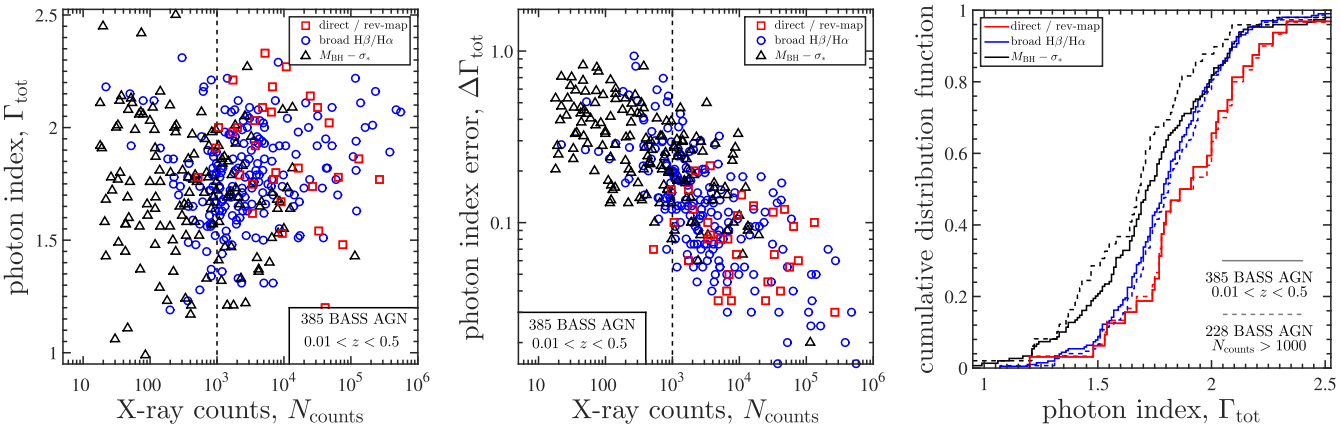

Figure 1. Statistical properties of the hard X-ray photon index, Γ_x, in our AGN sample. *Left*: the best-fitting photon index over the entire available range of X-ray data, Γ_{tot}, versus the number of counts in this energy range, N_{counts}. Our AGNs are split according to the M_{BH} (and therefore L/L_{Edd}) determination method: either through 'direct' methods (masers, resolved gas or stellar kinematics, or reverberation; red squares); through 'single-epoch' mass estimators using one of the broad Balmer lines (blue circles); or through stellar velocity dispersions (σ_*) and the M_{BH}–σ_* relation (black triangles). The dashed vertical line denotes $N_{counts} = 1000$ – the conservative threshold we apply to the parent BASS sample to focus on high-quality X-ray data. *Centre*: the uncertainty on the photon index, $\Delta\Gamma_{tot}$, versus N_{counts}. *Right*: cumulative distribution function of Γ_{tot}. Lines of different colours trace the M_{BH} subsets. For each subset, solid and dashed lines trace the distribution of Γ_{tot} among all AGN and among those with $N_{counts} > 1000$, respectively.

For 149 AGN, our M_{BH} estimates rely on single-epoch spectra of the broad Balmer emission lines, and prescriptions that fundamentally rely on the results of reverberation mapping campaigns. In particular, for 126 sources, we used the broad Hβ emission line and the adjacent continuum luminosity ($L_{5100} \equiv \lambda L_\lambda[5100\,\text{Å}]$, relying on the same line fitting procedure and M_{BH} estimator as in Trakhtenbrot & Netzer (2012). For 23 additional sources, M_{BH} is determined from the broad Hα emission line, following the procedure described in Oh et al. (2015) and the prescription of Greene & Ho (2005). Finally, for 49 sources with no broad emission lines, we used σ_* measurements and the M_{BH}–σ_* relation of Kormendy & Ho (2013).

As explained in the BASS/DR1 paper (K17), we prefer to use the 'direct' M_{BH} determinations, whenever available. Otherwise, we use the single-epoch estimates from broad Balmer lines, and finally those from σ_*. This reflects the different levels of uncertainty related to each of the mass estimation methods, which are discussed in K17. We briefly note here that the uncertainties on BH masses derived through single-epoch spectra of broad lines – which constitute the largest subset in our BASS sample – may reach ∼0.3–0.4 dex (see e.g. Shen & Liu 2012; Shen 2013; Peterson 2014; Mejía-Restrepo et al. 2016, and references therein). On the other hand, for M_{BH} determinations based on resolved stellar or gas dynamics (including masers), the statistical uncertainties are much lower, $\lesssim$0.1 dex. Importantly, the single-epoch mass estimators are calibrated in a way that minimizes any systematic offsets with respect to other methods (see e.g. Park et al. 2012; Grier et al. 2013; Woo et al. 2013).

We estimated the bolometric luminosities of our sources, L_{bol}, following several different prescriptions, based on the available X-ray and optical luminosities of our AGN. We mainly use the (absorption-corrected) luminosities in the 2–10 keV rest-frame energy range, L_{2-10}, derived from the best-fitting, multicomponent spectral models of the X-ray data (but ignoring any cross-calibration scaling factors; see R17). These are combined with three different bolometric corrections. First, we used a fixed bolometric correction of $f_{bol,\,2-10\,keV} \equiv L_{bol}/L_{2-10} = 20$, a typical value for AGN (see e.g. Elvis et al. 1994; Marconi et al. 2004; Vasudevan & Fabian 2007; Jin et al. 2012). Second, we used the L_{2-10}-dependent bolometric corrections of Marconi et al. (2004). For the sample considered in this study, these are in the range of $f_{bol,\,2-10\,keV} = 11$–140, with a median value of $f_{bol,\,2-10\,keV} = 26.7$, and 80 per cent of the sources having $f_{bol,\,2-10\,keV} \simeq 18$–$48$. The resulting L_{bol} are therefore slightly larger than those obtained through $f_{bol,\,2-10\,keV} = 20$, by 0.1 dex (median value; the standard deviation is 0.18 dex), but otherwise there are no significant systematic differences between the two. We have also examined the effects that an L/L_{Edd}-based bolometric correction would have on our results. For this, we relied on the results of Vasudevan & Fabian (2007), which provide $f_{bol,\,2-10\,keV} = 20$ for $L/L_{Edd} \leq 0.04$, $f_{bol,\,2-10\,keV} = 70$ for $L/L_{Edd} \geq 0.4$, and follow $f_{bol,\,2-10\,keV} \propto L/L_{Edd}^{0.54}$ over the range $0.04 < L/L_{Edd} < 0.4$. The more recent study of Jin et al. (2012) suggests a similar dependence of f_{bol}.[2] We stress that these prescriptions for L_{bol} may provide markedly different values for individual sources, and therefore potentially affect any analysis of the Γ_x–L/L_{Edd} plane. We indeed consider them all in our analysis (see Section 3.2).

We additionally used the absorption-corrected BAT luminosities, which cover the range 14–150 keV, combined with a fixed bolometric correction of $f_{bol,\,14-150\,keV} \equiv L_{bol}/L_{BAT} = 8.5$. This bolometric correction is derived from the $f_{bol,\,2-10\,keV} = 20$ one, by assuming a constant $\Gamma_x = 1.8$ – similar to the median value our sample (see Fig. 1), which corresponds to $L_{BAT}/L_{2-10} = 2.35$. These L_{BAT}-based estimates of L_{bol} are generally in very good agreement with the fiducial, L_{2-10}-based ones. The median difference is 0.04 dex (with L_{BAT}-based estimates of L_{bol} being slightly lower), and the standard deviation is 0.21 dex.

Finally, for the subset of 126 AGN for which M_{BH} was determined from single-epoch spectroscopy of the broad Hβ line, we derived an additional set of L_{bol} estimates using L_{5100}-dependent bolometric corrections, $f_{bol}(5100\,\text{Å})$, which are calibrated against the Marconi et al. (2004) ones (see also Trakhtenbrot & Netzer 2012). In the range of L_{5100} covered by our BASS sample, these can be approximated by

[2] It has been suggested that the $f_{bol,\,2-10\,keV}$–L/L_{Edd} relation is itself a reflection of an underlying Γ_x–L/L_{Edd} positive correlation (e.g. Fanali et al. 2013).

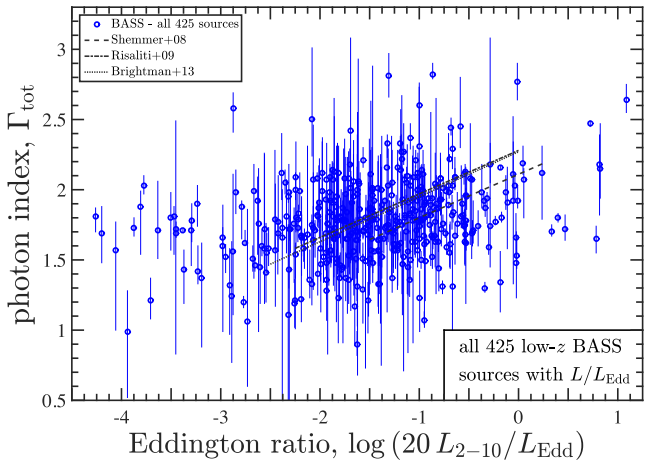

Figure 2. $\Gamma_{\rm tot}$ versus $L/L_{\rm Edd}$ for the parent raw sample of 425 BASS AGN – ignoring restrictions on the number of X-ray counts ($N_{\rm counts}$) or on the lower redshift bound. The grey diagonal lines represent the best-fitting $\Gamma_{\rm x}$–$L/L_{\rm Edd}$ relations reported by the studies of Shemmer et al. (2008), Risaliti et al. (2009), and Brightman et al. (2013), over the (approximate) range covered by the respective samples.

$\log f_{\rm bol}(5100\,\text{Å}) = -0.084 \times \log(L_{5100}/10^{44}\,{\rm erg\,s^{-1}}) + 0.9$. This set of $L/L_{\rm Edd}$ estimates is mainly used to allow a direct comparison with the analysis presented in some previous studies of the $\Gamma_{\rm x}$–$L/L_{\rm Edd}$ relation (e.g. S08; see Section 4.2).

Throughout this work, we focus mainly on the L_{2-10}-based determinations of $L_{\rm bol}$ (and therefore $L/L_{\rm Edd}$). This choice is mainly motivated by our attempt to minimize the effects of source variability on our measurements and analysis. The lower energy X-ray data, which dominate the determination of $\Gamma_{\rm x}$ (and, obviously, of L_{2-10}), were obtained through integrations that are much shorter than the *Swift*/BAT ones (which, in turn, represent typical flux levels over a period of ∼70 months). The Eddington ratios of our AGN, which provide a dimensionless, $M_{\rm BH}$-normalized measure of the accretion rate on to the SMBHs, are then calculated following $L/L_{\rm Edd} = L_{\rm bol}/(1.3 \times 10^{38}\,M_{\rm BH}/M_{\odot})$.

3 THE $\Gamma_{\rm x}$–$L/L_{\rm Edd}$ RELATION FOR *Swift*/BAT AGN

3.1 Straightforward analysis with $\Gamma_{\rm tot}$–$L/L_{\rm Edd}$

Fig. 2 shows the photon index versus the accretion rate for the entire (parent) sample of 425 BASS AGN. We stress that this includes *all* the non-blazar sources for which the quantities are available, ignoring (for now) the different redshift and $N_{\rm counts}$ cuts described above, and regardless of the method used for $M_{\rm BH}$ estimation. Here, we use the photon index we obtained from the entire spectral fit to the available X-ray data, $\Gamma_{\rm tot}$, and the $L/L_{\rm Edd}$ estimates that are based on $L_{\rm bol} = 20 \times L_{2-10}$.

A formal (Spearman) hypothesis test results in a weak and only marginal statistically significant correlation between the quantities, with the probability of finding a correlation if the null hypothesis (i.e. no correlation) is true being $P = 0.8$ per cent, and a correlation coefficient of $r_{\rm s} = 0.23$.[3] Thus, it appears that our parent BASS sample may hold limited evidence for a $\Gamma_{\rm x}$–$L/L_{\rm Edd}$ relation of the kind found in several previous studies, although at lower statistical significance ($<3\sigma$). However, in what follows we will demonstrate that this result is not robust, and in particular that it does not hold for subsets of sources that differ in the $M_{\rm BH}$ determination methodology, for alternative determinations of $L/L_{\rm Edd}$, and/or when some data quality cuts are imposed on the sample.

In Fig. 3, we again show $\Gamma_{\rm tot}$ versus $L/L_{\rm Edd}$, but only for the 228 BASS AGN in our main sample, i.e. those that satisfy $N_{\rm counts} > 1000$ and $0.01 < z < 0.5$. Here, too, we use $\Gamma_{\rm tot}$ and the L_{2-10}-based estimates of $L/L_{\rm Edd}$. Fig. 3 also shows the best-fitting relations between $\Gamma_{\rm x}$ and $L/L_{\rm Edd}$ reported in the three main reference studies of S08, R09, and B13. Adopting a notation of

$$\Gamma_{\rm x} = \alpha\,\log(L/L_{\rm Edd}) + \beta, \quad (1)$$

these studies have reported $(\alpha, \beta) = (0.31, 2.11)$, $(0.31, 2.28)$, and $(0.32, 2.27)$, respectively.[4] The samples and methods used in these studies are described in Section 4.2.

As Fig. 3 clearly shows, there is a considerable amount of scatter and little evidence for strong trends between $\Gamma_{\rm tot}$ and $L/L_{\rm Edd}$ in our sample of 228 BASS AGN. In an attempt to illustrate the overall trends that may be present in our sample, in Fig. 4 we show the *binned* $\Gamma_{\rm x}$ versus $L/L_{\rm Edd}$ for each of the $M_{\rm BH}$ subsets, where the bins spread 0.5 dex in $L/L_{\rm Edd}$. The markers represent the median values within each bin, while the vertical error bars represent the median absolute deviations (MAD) of $\Gamma_{\rm tot}$. Fig. 4 further demonstrates the large scatter in the (underlying) BASS sample, and the limited evidence for a strong $\Gamma_{\rm x}$–$L/L_{\rm Edd}$ correlation for our AGN. A formal correlation test does indeed show evidence for a weak, but statistically significant correlation: the null hypothesis of no correlation between $\Gamma_{\rm tot}$ and $L/L_{\rm Edd}$ can be rejected at a level corresponding to $P = 1.65 \times 10^{-4}$ per cent, when the entire sample of 228 AGN is considered. The corresponding Spearman correlation coefficient is $r_{\rm s} = 0.31$ – implying a weak correlation.[5] The results of this and other correlation tests are given in Table 1.

We employ several linear regression analysis methods to derive the best-fitting parameters of the $\Gamma_{\rm tot}$–$L/L_{\rm Edd}$ correlation for the primary BASS sample. In all these fits, we assume a uniform uncertainty of 0.3 dex on $L/L_{\rm Edd}$ (following S08). The BCES(Y|X) method (Akritas & Bershady 1996) provides

$$\Gamma_{\rm tot} = (0.167 \pm 0.04)\,\log(L/L_{\rm Edd}) + (2.00 \pm 0.05), \quad (2)$$

while the BCES bisector fit[6] provides $\alpha = 0.444 \pm 0.060$ and $\beta = 2.34 \pm 0.077$. The FITEXY method, adapted to include intrinsic scatter (following Tremaine et al. 2002), provides $\alpha = 0.167 \pm 0.029$ and $\beta = 2.004 \pm 0.038$ (and an intrinsic scatter of 0.24) – in excellent agreement with the BCES(Y|X) result. Fig. 3 presents the BCES bisector and FITEXY best-fitting relations. Table 2 lists the best-fitting parameters for all three linear fits, as

[3] Throughout this work, we define a correlation as 'significant' if the *two-sided* Spearman correlation test results in $P < 0.1$ per cent (corresponding to $>3.3\sigma$). Correlations with $0.1 < P < 1$ per cent (i.e. $\sim 2.6\sigma$–3.3σ) are referred to as 'marginally significant', in order to avoid a situation where small differences in P-values result in stark qualitative disagreements with previous works.

[4] For the R09 study, we list the relation which relies on the 'total' sample, despite the fact that for ∼17 per cent of those AGN have C IV λ1549-based determinations of $M_{\rm BH}$ (and therefore, $L/L_{\rm Edd}$), which are known to be problematic (see Trakhtenbrot & Netzer 2012, and references therein). The relation derived in R09 for AGN with Hβ-based determinations of $M_{\rm BH}$ is much steeper, with $(\alpha, \beta) = (0.58, 2.57)$.

[5] We stress that this value of the correlation coefficient $r_{\rm s}$ should *not* be directly compared with the slopes of the $\Gamma_{\rm x}$–$L/L_{\rm Edd}$ relations reported by the aforementioned studies, despite their similarity.

[6] All our BCES fits used 1000 realizations of the relevant data sets.

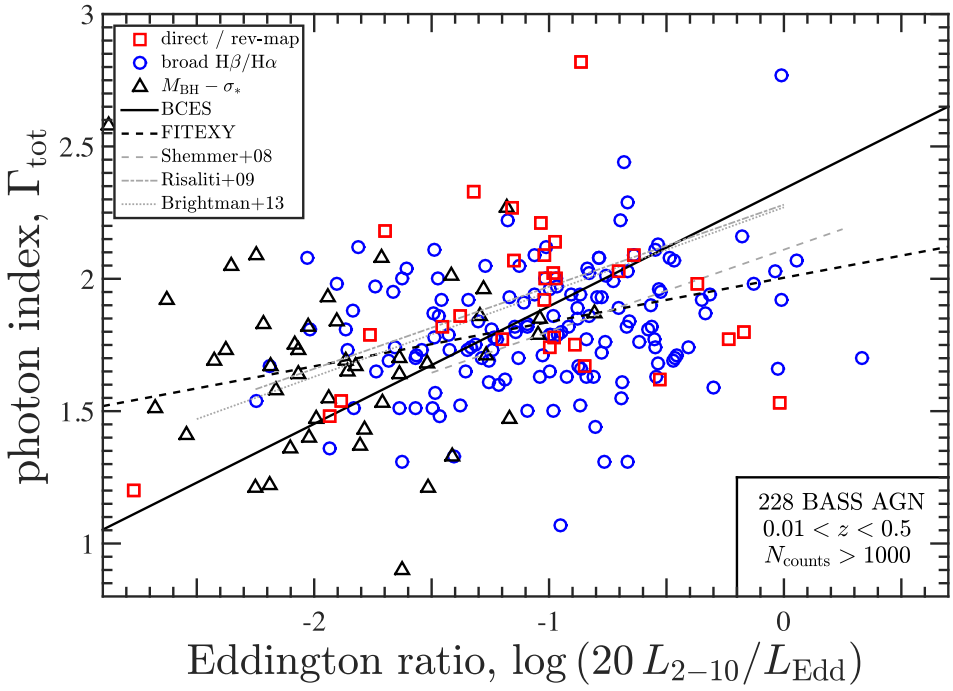

Figure 3. Γ_{tot} versus L/L_{Edd} for our sample of 228 BASS AGN with $0.01 < z < 0.5$ and high-quality X-ray data ($N_{counts} > 1000$). Different symbols represent AGN for which M_{BH} (and therefore L/L_{Edd}) is estimated either through 'direct' methods (masers, resolved gas or stellar kinematics, or reverberation); through 'single-epoch' mass estimators using one of the broad Balmer lines; or through stellar velocity dispersions (σ_*) and the M_{BH}–σ_* relation. The black diagonal lines represent the best-fitting Γ_{tot}–L/L_{Edd} relations we obtain using either the BCES (bisector) or the FITEXY methods (solid and dashed lines, respectively). The grey diagonal lines represent the best-fitting Γ_x–L/L_{Edd} relations reported by the studies of Shemmer et al. (2008), Risaliti et al. (2009), and Brightman et al. (2013), over the (approximate) range covered by the respective samples.

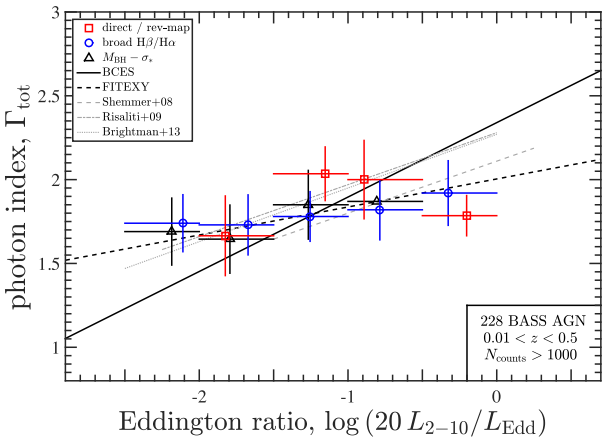

Figure 4. Same as Fig. 3, but binning the AGN in each M_{BH} subset according to L/L_{Edd}, in steps of 0.5 dex. Markers represent the median L/L_{Edd} and Γ_{tot} in each such bin. Error bars on L/L_{Edd} represent the bin size, while those on Γ_x represent the MAD. All symbols and lines are identical to those in Fig. 3 (the black lines represent the best-fitting relations obtained for the unbinned data).

well for the other statistically significant Γ_x–L/L_{Edd} correlations we find for the primary BASS sample of 228 sources (i.e. those with $P < 0.1$ per cent). We also tabulate the standard deviation of the residuals (i.e. $\sigma[\Gamma_x^{obs} - \Gamma_x^{fit}]$). We note that in fitting this Γ_x–L/L_{Edd} relation, as well as in virtually all other cases, the best-fitting BCES bisector linear regression diverges from the two other methods, and the resulting residuals show significant trends with L/L_{Edd}.

We highlight the fact that the best-fitting Γ_x–L/L_{Edd} relations we find using the consistent BCES(Y|X) and FITEXY(Y|X) methods suggest much weaker dependence of Γ_x on L/L_{Edd}, compared to those reported in previous studies (i.e. $\alpha \simeq 0.16$ versus $\sim$0.31). Moreover, these linear relations fail to reduce the considerable amount of scatter in the Γ_{tot}–L/L_{Edd} plane: the standard deviations of the residuals, roughly $\sigma(\Delta) \gtrsim 0.25$, are comparable to the general standard deviation of Γ_{tot} in our sample ($\sigma[\Gamma_{tot}] = 0.27$). Thus, there is little evidence that these linear relations provide a preferred description of the Γ_{tot}–L/L_{Edd} parameter space, and/or the range in Γ_{tot} seen in the BASS sample.

Despite the statistically significant (though weak) Γ_{tot}–L/L_{Edd} correlation found for the primary BASS sample as a whole, a closer inspection of the three different M_{BH} subsets provides very limited evidence for such correlations within these subsets. In particular, the subsets with 'direct', 'single-epoch', and 'σ_*' determinations of M_{BH} result in P-values of 94.6 per cent, 0.36 per cent, and 39.2 per cent, respectively (all based on Spearman correlation tests; see Table 1). We highlight the lack of a statistically significant correlation among the most reliable M_{BH} determinations (i.e. the 'direct' subset) and the weak evidence for a correlation among the single-epoch subset, which most closely resembles the M_{BH} estimation methodology of the aforementioned reference studies.

These apparently qualitatively inconsistent results – for the BASS sample as a whole and for the different M_{BH} subsets – suggest that the correlation between Γ_{tot} and L/L_{Edd} may not be robust nor universal. We discuss this further in Section 4.

3.2 Examining alternative determinations of Γ_x and/or L/L_{Edd}

We next examine the alternative determinations of Γ_x and L/L_{Edd} available for our sample, to further test whether we can establish any

Table 1. BASS Γ_X–L/L_{Edd} correlations: significance tests. Statistically significant *P*-values are highlighted in bold.

L_{bol} tracer	Γ	Sub-sample	N	P-value (per cent)	r_s
$C \cdot L_{2-10}$	Γ_{tot}	All, $0.01 < z < 0.5$	228	$\mathbf{1.7 \times 10^{-4}}$	0.311
		Direct M_{BH}	30	94.6	0.013
		Single-epoch M_{BH}	149	0.36	0.237
		σ_*-based M_{BH}	49	39.2	0.125
$C \cdot L_{2-10}$	$\Gamma_{0.3-10}$	All, $0.01 < z < 0.5$	228	$\mathbf{1.2 \times 10^{-4}}$	0.315
		Direct M_{BH}	30	66.8	0.082
		Single-epoch M_{BH}	149	1.31	0.203
		σ_*-based M_{BH}	49	67.4	−0.062
$C \cdot L_{2-10}$	Γ_{nEc}	All, $0.01 < z < 0.5$	228	$\mathbf{3.9 \times 10^{-7}}$	0.377
		Direct M_{BH}	30	78.5	0.052
		Single-epoch M_{BH}	149	$\mathbf{1.1 \times 10^{-2}}$	0.311
		σ_*-based M_{BH}	49	40.7	0.121
$C \cdot L_{2-10}$	Γ_{BAT}	All, $0.01 < z < 0.5$	228	$\mathbf{2.0 \times 10^{-8}}$	0.405
		Direct M_{BH}	30	4.00	0.377
		Single-epoch M_{BH}	149	0.16	0.256
		σ_*-based M_{BH}	49	40.8	0.121
f_{bol}[M04] $\cdot L_{2-10}$	Γ_{tot}	All, $0.01 < z < 0.5$	228	$\mathbf{8.7 \times 10^{-5}}$	0.319
		Direct M_{BH}	30	84.2	0.038
f_{bol}[VF07] $\cdot L_{2-10}$	Γ_{tot}	All, $0.01 < z < 0.5$	228	$\mathbf{1.6 \times 10^{-4}}$	0.311
		Direct M_{BH}	30	94.6	0.013
$C \cdot L_{BAT}$	Γ_{tot}	All, $0.01 < z < 0.5$	228	0.39	0.190
		Direct M_{BH}	30	48.4	−0.133
f_{bol}[M04] $\cdot L_{5100}$	Γ_{tot}	Single-epoch, Hβ	126	0.11	0.287
AGN property	Γ	Sub-sample	N	P-value	r_s
L_{2-10}	Γ_{tot}	All, $0.01 < z < 0.5$	228	2.43	0.149
L_{BAT}				85.3	−0.012
M_{BH}				3.27	−0.142
FWHM(Hβ/Hα)			149	84.3	−0.013

Table 2. BASS Γ_X–L/L_{Edd} correlations: best-fitting parameters.

L_{bol} tracer	Γ	BCES (bisector)			BCES (Y|X)			FITEXY			
		α	β	$\sigma(\Delta)$	α	β	$\sigma(\Delta)$	α	β	ϵ	$\sigma(\Delta)$
$C \cdot L_{2-10}$	Γ_{tot}	0.444 ± 0.060	2.34 ± 0.07	0.33	0.167 ± 0.040	2.00 ± 0.05	0.26	0.167 ± 0.029	2.00 ± 0.04	0.24	0.26
	$\Gamma_{0.3-10}$	0.601 ± 0.096	2.46 ± 0.12	0.45	0.130 ± 0.050	1.89 ± 0.07	0.30	0.154 ± 0.029	1.93 ± 0.04	0.24	0.30
	Γ_{nEc}	0.364 ± 0.150	2.30 ± 0.18	0.30	0.159 ± 0.031	2.06 ± 0.18	0.26	0.158 ± 0.029	2.05 ± 0.04	0.24	0.26
	Γ_{BAT}	-0.278 ± 0.070	1.64 ± 0.09	0.35	0.160 ± 0.023	2.17 ± 0.03	0.21	0.204 ± 0.018	2.18 ± 0.03	0.04	0.22
f_{bol}[M04] $\cdot L_{2-10}$	Γ_{tot}	0.395 ± 0.060	2.23 ± 0.07	0.33	0.143 ± 0.032	1.96 ± 0.04	0.26	0.148 ± 0.023	1.97 ± 0.03	0.22	0.26
f_{bol}[VF07] $\cdot L_{2-10}$	Γ_{tot}	0.339 ± 0.048	2.11 ± 0.05	0.33	0.116 ± 0.026	1.91 ± 0.03	0.26	0.120 ± 0.019	1.91 ± 0.02	0.22	0.26

(stronger) relations between these quantities. In particular, we have examined relations between the L_{2-10}-based estimates of L/L_{Edd} (and $f_{bol,\,2-10\,keV} = 20$), and either $\Gamma_{0.3-10}$, Γ_{BAT}, or Γ_{nEc} – shown in Fig. 5. We have also used the alternative set of L/L_{Edd} estimates, in which L_{bol} is estimated from L_{2-10} and the bolometric corrections of either Marconi et al. (2004), or those of Vasudevan & Fabian (2007) – presented in the top two panels of Fig. 6. The L_{BAT}-based estimates of L/L_{Edd} (i.e. $L_{bol} = 8.5\,L_{BAT}$) are presented in the bottom-left panel of Fig. 6, while the bottom-right panel presents the L_{5100}-based estimates of L/L_{Edd}, for the subset of 126 AGN for which M_{BH} is determined from single-epoch spectroscopy of the broad Hβ line.

The results of all these tests are qualitatively similar to our main analysis of Γ_{tot} versus $L/L_{Edd}(L_{2-10})$: large scatter, statistically significant correlations between Γ_X and L/L_{Edd} for the overall primary BASS sample (i.e. 228 AGN), but no correlation within any of the three M_{BH} subsets – as can be seen in the results of the formal correlation analyses (listed in Table 1). We particularly note that in all the cases we examined (i.e. all L/L_{Edd}), the most reliable 'direct' M_{BH} subset did *not* result in statistically significant correlations. The 'single-epoch' subset shows somewhat stronger evidence for correlations, with *P*-values $\lesssim 1$ per cent in all cases, and a statistically significant (but weak) correlation for the case where Γ_{nEc} is considered ($P \simeq 10^{-2}$ per cent, $r_s = 0.31$; the best-fitting (FITEXY) relation has $\alpha = 0.16$). Another noteworthy exception is the lack of correlation between Γ_{tot} and the L_{BAT}-based determinations of L/L_{Edd}, even among the entire primary BASS sample (bottom panel of Fig. 3). Importantly, we find that the correlation between Γ_{tot}- and the L_{5100}-based estimates of L/L_{Edd}, for the subset of AGN with single-epoch, broad Hβ determinations of M_{BH}, is neither truly statistically significant ($P = 0.11$ per cent) nor strong ($r_s = 0.29$). We will revisit this subset when comparing our results with previous studies of the Γ_X–L/L_{Edd} relation (see Section 4.2).

We finally note that the BASS sample provides no compelling evidence for an 'inversion' of the Γ_X–L/L_{Edd} relation for low-L/L_{Edd}

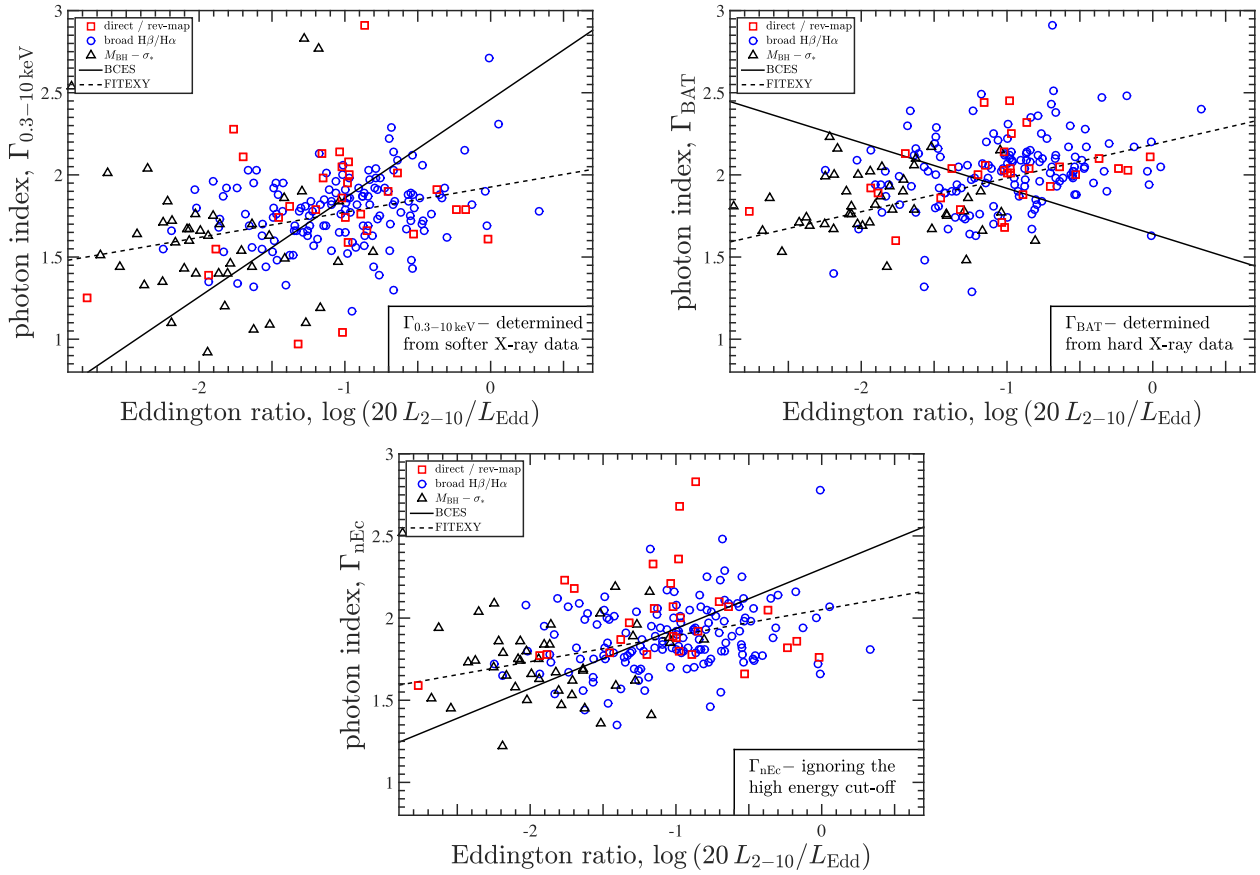

Figure 5. Same as Fig. 3, but with alternative determination of the photon index, Γ_x. *Top left*: $\Gamma_{0.3-10}$ – obtained from the full X-ray spectral model, fitted over the energy range 0.3–10 keV. *Top right*: Γ_{BAT} – obtained from a power-law spectral model fitted over the *Swift*/BAT energy range of 14–195 keV. *Bottom*: Γ_{nEc} – obtained from a modified spectral model that ignores the high-energy exponential cut-off.

systems (i.e. changing into an anticorrelation for $L/L_{Edd} \ll 0.01$), as suggested by some studies (e.g. Younes et al. 2011; Gültekin et al. 2012; Kamizasa et al. 2012; Yang et al. 2015; Kawamuro et al. 2016b). Motivated by these claims, we also explicitly verified that the high-L/L_{Edd} regime in our sample (AGN with $L/L_{Edd} > 0.01$) does not present a strong, underlying Γ_x–L/L_{Edd} correlation which is then 'diluted' by the lower L/L_{Edd} sources (see Section 3.3 below and Appendix A).

3.3 Additional tests for subsets of AGN

Finally, we examined several subsets of sources within our BASS sample, verifying that none of the choices we made in defining our sample, or our treatment of certain physically motivated spectral components, would have a significant effect on our conclusion. In particular, we tested for the existence of Γ_x–L/L_{Edd} correlations among: AGN with $0.05 < z < 0.5$ – minimizing aperture effects; AGN with high-quality (SDSS) optical spectra; AGN with $0.01 < L/L_{Edd} < 1$; AGN with no heavy obscuration ($\log(N_H/cm^{-2}) < 23$); and AGN without warm absorbers. These subsets are described in Appendix A, and the results of the correlation tests are tabulated in Table A1). The qualitative results of this analysis are consistent with what we find for the primary BASS sample: for each subset, we find either no correlation, or alternatively, a weak correlation for all the AGN in that subset, while finding no correlations among sources with differing M_{BH} determination methods.

3.4 Relations between Γ_x and other AGN properties

We looked for relations between Γ_x and other key properties of the accreting SMBHs in our sample. Fig. 7 presents Γ_{tot} versus L_{2-10}, FWHM(Hβ) (or Hα), and M_{BH}.[7] The P-values associated with these correlation tests are listed in Table 1. None of these relations resulted in a statistically significant correlation. A qualitatively similar result was obtained when testing for correlations involving $\Gamma_{0.3-10}$ or Γ_{nEc}. These results are in agreement with the findings of previous studies that investigated possible links between Γ_x and other AGN properties.

The broad dynamical range in L_{2-10}, L_{bol}, M_{BH}, and L/L_{Edd} covered by our sample allows us to further investigate whether the mutual dependence between (some of) these quantities has any effects on the Γ_x–L/L_{Edd}. To this end, we examined subsets of our sample for which one of these properties is controlled. Considering only the AGN with $\log(L_{2-10}/erg\,s^{-1}) = 43.25$–$43.75$ (i.e. a bin of ±0.25 dex around the median luminosity, with 71 sources), we find no evidence for a significant Γ_x–L/L_{Edd} correlation ($P = 2$ per cent for Γ_{tot}, and >0.1 per cent for all other cases). This should be compared to the highly significant correlations found when considering the entire luminosity range ($P \ll 10^{-3}$ per cent in all cases; see Table 1). A similar analysis for AGN with

[7] For the purposes of the test with the FWHM of broad Balmer lines, we focused only on the 149 AGN with single-epoch determinations of M_{BH} (i.e. ignoring the 30 AGN with 'direct' mass measurements).

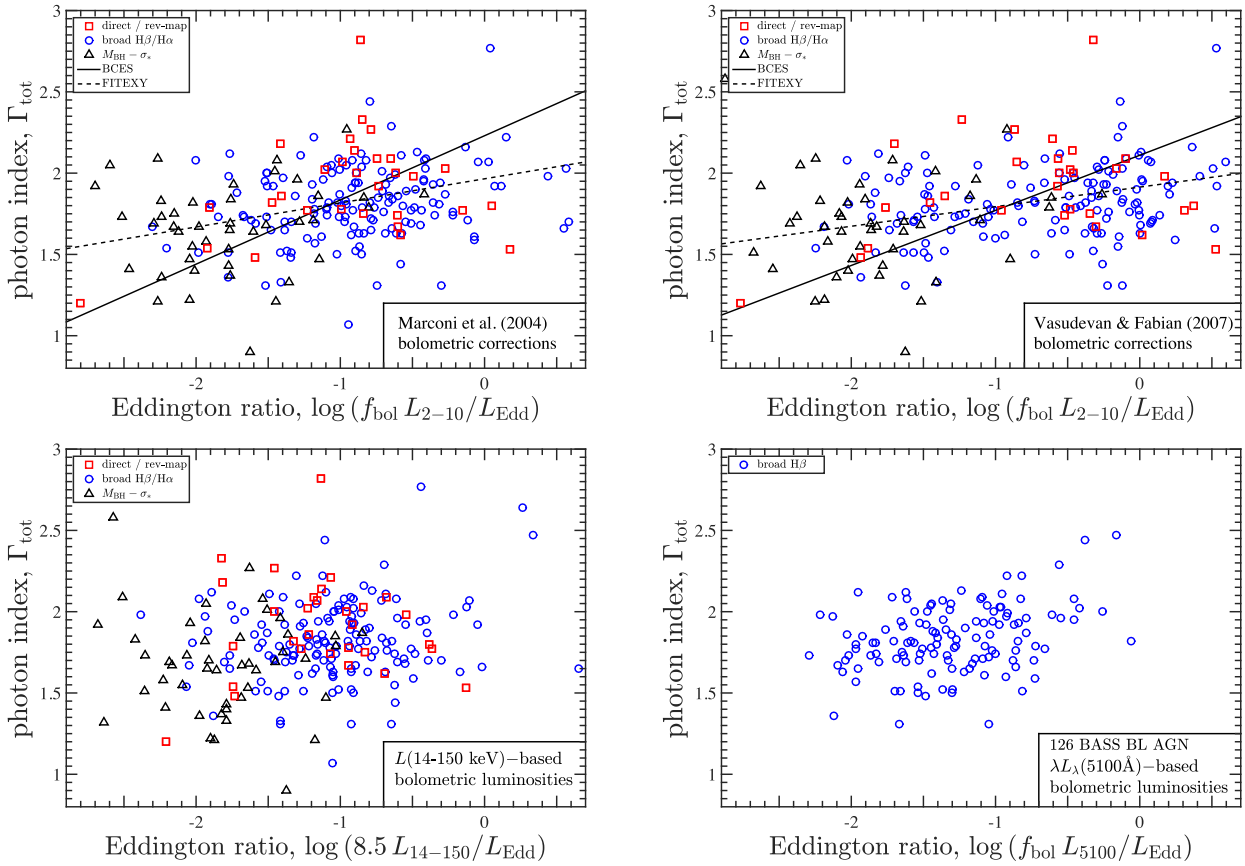

Figure 6. Same as Fig. 3, but with alternative determination of the accretion rate, L/L_{Edd}. The symbols in all panels are as in Figs 3–5. Black diagonal lines represent the best-fitting correlations (using either the BCES bisector or the FITEXY methods), for the cases where the Γ_x–L/L_{Edd} correlation is statistically significant. *Top*: Γ_{tot} versus L/L_{Edd} estimates derived from L_{2-10}, and through either the L_{2-10}-dependent bolometric corrections of Marconi et al. (2004, *left*), or the L/L_{Edd}-dependent bolometric corrections of Vasudevan & Fabian (2007, *right*). *Bottom left*: Γ_{tot} versus L/L_{Edd} estimates derived through $L_{bol} = 8.5 \times L_{BAT}$. *Bottom right*: Γ_{tot} versus L/L_{Edd} estimates derived from L_{5100}, and through L_{5100}-dependent bolometric corrections (calibrated against those of Marconi et al. 2004; see Section 2.3), for the subset of 126 AGN with single-epoch, broad Hβ determinations of M_{BH}. In these two cases, we find no statistically significant correlations.

$\log(M_{BH}/M_\odot) = 7.75$–$8.25$ (again within ± 0.25 dex of the median value; 64 sources) provides a qualitatively different result: the statistically significant Γ_x–L/L_{Edd} correlation holds for most cases ($P \simeq 0.1$ per cent for Γ_{tot} and $\Gamma_{0.3-10}$; $<10^{-3}$ per cent for Γ_{nEc} and Γ_{BAT}). We stress that these two special subsets of AGN cover the same range in both L/L_{Edd} and Γ_x as does our primary BASS sample. This is only possible thanks to the broad range of L/L_{Edd} and M_{BH} provided through the BASS project (see K17).

These results, together with the fact that L/L_{Edd} is strongly correlated with L_{2-10} in our sample ($P \simeq 10^{-3}$ per cent, $r_s = 0.29$), suggest that the Γ_{tot}–L/L_{Edd} relation for the primary BASS sample may be – at least partially – driven by the trend with source luminosity.

4 DISCUSSION

4.1 The BASS $\Gamma_x - L/L_{Edd}$ plane for different classes of AGN

Our analysis shows no evidence for a robust Γ_x–L/L_{Edd} relation among the subsets of AGN for which reliable estimates of M_{BH} (and therefore, of L/L_{Edd}) are available, while *also* showing evidence for a significant correlation among the BASS sample as a whole, as well as (marginal) evidence for a correlation among the broad-line sources. How could these qualitatively contradicting results be reconciled?

The study of Winter et al. (2012) has identified a similar discrepancy, when finding a strong Γ_x–L/L_{Edd} correlation *only* among the broad-line *Swift*/BAT-selected AGN in their sample. The interpretation put forward by that study suggested that the lower luminosity and/or lower L/L_{Edd}, absorbed AGN are found in a different accretion state. For our BASS sample, a closer inspection of Figs 1 and 3, suggests that the σ_* subset (i.e. AGN with no broad Balmer lines, and no direct M_{BH} determination) exhibits somewhat lower Γ_x, compared with the other two M_{BH} subsets (see also Vasudevan, Mushotzky & Gandhi 2013). In addition, the studies of Fabian, Vasudevan & Gandhi (2008) and Fabian et al. (2009) showed that such narrow-line sources are predominantly low-L/L_{Edd} systems. The combined effect of these two trends is that the σ_* subset mainly extends towards the low-L/L_{Edd}, low-Γ_x part of the parameter space, which in turn results in statistically significant Γ_x–L/L_{Edd} correlations once this subset is included in the analysis.

Are these two trends driven by physical processes or by observational limitations (i.e. selection effects)? As suggested by Fabian et al. (2008), the tendency of obscured (narrow line) AGN towards low L/L_{Edd} is likely driven by the limited radiation pressure that low-L/L_{Edd} AGN exert on the surrounding dusty circumnuclear gas

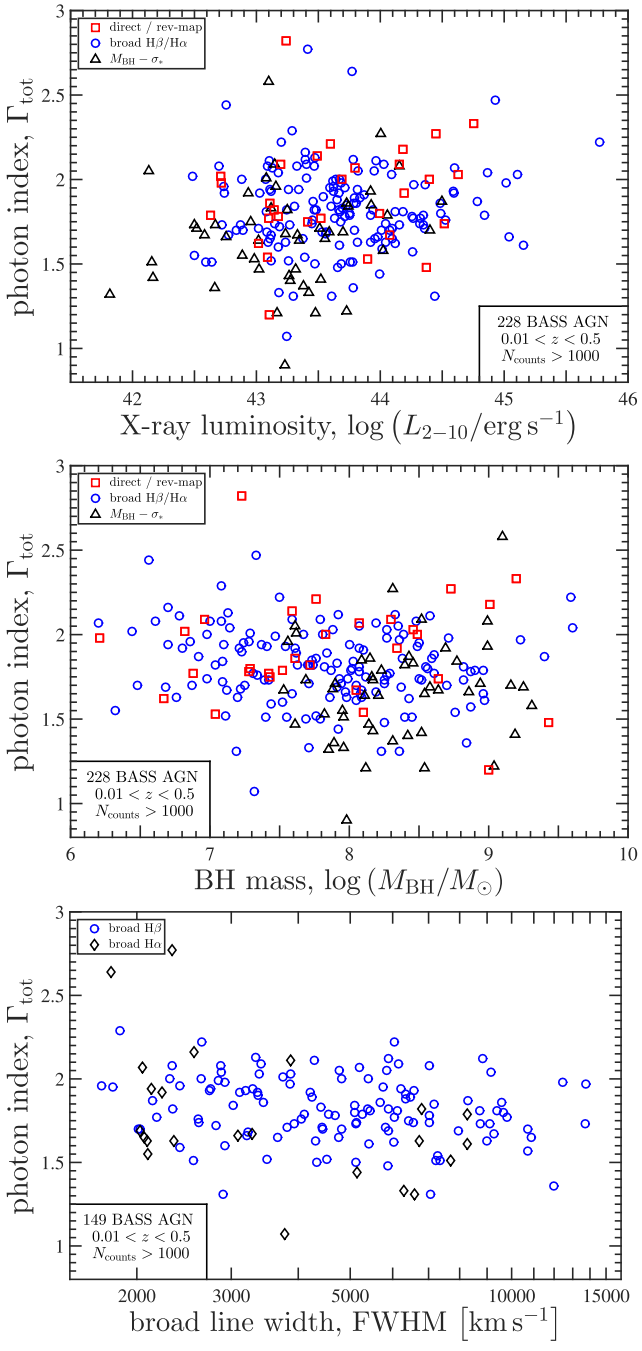

Figure 7. Testing for relations between X-ray photon index Γ_{tot} and other key AGN properties. *Top*: Γ_{tot} versus hard X-ray luminosity (14–150 keV) probed by *Swift*/BAT, L_{BAT}. *Centre*: Γ_{tot} versus BH mass, M_{BH}. In both these panels, symbols are identical to Fig. 3. *Bottom*: Γ_{tot} versus width of the broad Balmer lines (Hβ or Hα) for those sources for which these data are available. No correlations are found between Γ_{tot} and any of these properties.

(i.e. the dusty tori), which in turn result in increased levels of optical and X-ray obscuration. This issue is investigated in detail, in the context of the BASS sample and data, in a forthcoming study by Ricci et al.

The outstanding question is therefore whether the somewhat lower Γ_x seen in obscured AGN is *driven* by the Γ_x–L/L_{Edd} correlation (the origin of which not yet well understood; see below), or rather by an unrelated physical and/or observational effect, which – when combined with the tendency of obscured AGN to have lower L/L_{Edd} – *produces* the observed Γ_x–L/L_{Edd} relation for our entire sample of BASS sources. One such scenario would be if obscured AGN have multiple partially covering (i.e. clumpy) absorption components (e.g. Cappi et al. 1996). In such a case, the measured Γ_x might be flatter than the real underlying photon index. Thus, a scenario in which the lower Γ_x of obscured sources is driven by physical effects beyond the Γ_x–L/L_{Edd} correlation would require that many (or indeed, most) obscured sources would have (at least) two partially covering absorbing components. This is, arguably, a rather extreme scenario.

4.2 Comparison with previous studies

We demonstrated that our sample of 228 low-redshift, hard X-ray-selected AGN shows no significant evidence for a correlation between the hard X-ray photon index, Γ_x, and the normalized accretion rate, L/L_{Edd}, nor with other key AGN properties such as BH mass (M_{BH}) and/or hard X-ray luminosity (L_{BAT}). This stands in contrast to the findings of several studies. In what follows, we briefly summarize three such studies, which form the main reference for our comparison.

(i) Shemmer et al. (2008, S08) studied 35 high-luminosity, high-redshift quasars (at $z \sim 0$–3.5), for which the X-ray spectral analysis mostly relied on *XMM-Newton* data in the observed-frame energy range 0.5–10 keV. BH masses were determined from broad Hβ spectroscopy, using the same prescription we use here, and L/L_{Edd} were calculated through the L_{5100}-dependent prescription of Marconi et al. (2004), consistent with the L_{5100}-dependent bolometric corrections we use here.

(ii) Risaliti et al. (2009, R09) analysed a sample of 343 moderate-to-high luminosity ($43 \lesssim \log[L_X/\mathrm{erg\,s^{-1}}] \lesssim 46.7$) SDSS quasars at $0.1 \lesssim z \lesssim 4.5$, with archival *XMM-Newton* data (compiled by Young, Elvis & Risaliti 2009). The X-ray spectra, covering 0.5–10 keV, were fitted with an (absorbed) power-law model. BH masses were determined from either the Hβ, Mg II λ2798, or C IV λ1549 broad emission lines (with 314 AGN having the more reliable Hβ- or Mg II-based masses). Bolometric luminosities were derived by using a fixed-shape UV-optical SED, and a power-law X-ray SED (with $E_C = 100$ keV). The Γ_x–L/L_{Edd} relations found for the subsets of AGN with either Hβ- or Mg II-based M_{BH} determinations are markedly different ($\alpha = 0.58$ and 0.24, respectively).

(iii) Brightman et al. (2013, B13) analysed a sample of 69 X-ray-selected, broad-line AGN from the *Chandra* surveys in the E-CDF-S and COSMOS fields, covering $0.5 \lesssim z \lesssim 2$ and $42.5 \lesssim \log[L_X/\mathrm{erg\,s^{-1}}] \lesssim 45.5$. The sample was restricted to sources with more than 250 counts in their spectra. BH masses were obtained through either Hα- or Mg II-based single-epoch estimators, which are generally consistent with those used here and in the other reference studies.

All these studies, which serve as primary reference studies for our work, focused on unobscured, broad-line AGN, for which M_{BH} is determined through single-epoch spectroscopy of broad emission lines – comparable to our 'single-epoch' M_{BH} subset. In addition, most of these studies employed a spectral model that includes only a single power law, with a minor absorption correction for a few sources.

The study of Winter et al. (2012) employed a more elaborate X-ray spectral model to a sample of broad-line *Swift*/BAT-selected AGN, and identified strong Γ_x–L_X and Γ_x–L/L_{Edd} relations, although the slope of the latter ($\alpha = 0.23$) is somewhat flatter than

what is found for the optically selected quasars mentioned above. More recently, the study of Brightman et al. (2016) studied the Γ_x–L/L_{Edd} relation in a sample of nine heavily obscured (mostly CT) AGN, for which precise M_{BH} measurements are available from resolved megamaser kinematics. This analysis resulted in a significant correlation with best-fitting parameters that are consistent with those derived in the aforementioned studies of unobscured AGN.

Comparing these reference studies to our BASS analysis, we first note the higher quality and broader energy coverage of our BASS X-ray data. These allow for a much more elaborate and robust spectral decomposition, taking into account several physically motivated components, and provide a set of various determinations of the key quantities (i.e. Γ_x and L_{bol}). We also note that our sample completely overlaps with the reference studies in terms of the range of Γ_x and L/L_{Edd} covered, and that it includes 174 broad-line AGN – the only class of AGN studied in the reference studies.

Although at face value our BASS analysis suggests a Γ_x–L/L_{Edd} correlation which is similar to those found in the reference studies, we note two main differences. First, we stress that we find little evidence for any Γ_x–L/L_{Edd} link among BASS sources for which M_{BH} is determined from single-epoch spectra of broad emission lines – the only subset comparable with the reference studies. Even for this subset, the only statistically significant correlation we find is when using Γ_{nEc} (which may be similar to the Γ_x used in some of the reference studies). Moreover, the correlation involving Γ_{BAT} – which could be thought of as comparable to what is measured for high-redshift sources (see S08) – is insignificant (although at $P = 0.16$ per cent). Second, the slopes of the best-fitting relations we derive for our *entire* BASS sample (Table 2) differ from those previously reported ($\alpha \simeq 0.3$): we find $\alpha \simeq 0.16$ for the ($\Gamma_x|L/L_{Edd}$) correlation analyses, but $\alpha \gtrsim 0.4$ for the BCES bisector. The discrepancy between the different fitting methods probably reflects the large scatter in the Γ_x–L/L_{Edd} plane.

To allow for a more direct comparison, we have derived yet another set of Γ_x measurements which aims to resemble the analysis performed in previous studies. We re-fitted the X-ray data of 162 BASS AGN that have $\log(N_H/cm^{-2}) \leq 22$ with a simplified spectral model of an absorbed power law over the rest-frame energy range 2–10 keV. By ignoring any additional components (i.e. warm absorbers, reflection, Fe Kα), this model – and the chosen energy range – are similar to what was used in the aforementioned reference studies. We stress that these derived photon indices, Γ_{simple}, are *not* identical to $\Gamma_{0.3-10}$ (see Section 2.2), despite the similarity in the respective energy ranges, as $\Gamma_{0.3-10}$ was derived from a more elaborate spectral model. We further focus on those AGN for which M_{BH} is determined through single-epoch spectroscopy of the broad Hβ emission line, and on the L_{5100}-based estimates of L/L_{Edd}.

Fig. 8 (top panel) plots these simplified photon indices (Γ_{simple}) against the L_{5100}-based estimates of L/L_{Edd} for the relevant 119 AGN in our sample. In this case, we find a statistically significant ($P \simeq 2 \times 10^{-3}$ per cent) yet, again, weak ($r_s = 0.383$) correlation between these two particular quantities. We recall that a similar analysis, with L_{5100}-based estimates of L/L_{Edd} for the single-epoch, broad-Hβ subset, but with Γ_{tot}, yielded only a marginally significant correlation ($P = 0.1$ per cent; see Section 3.2 and Fig. 6). A formal correlation analysis results in $(\alpha, \beta) = (0.906 \pm 0.11, 2.79 \pm 0.13)$, $(0.304 \pm 0.09, 2.00 \pm 0.13)$, and $(0.326 \pm 0.08, 2.03 \pm 0.10)$, for the BCES bisector, BCES(Y|X), and FITEXY methods, respectively (with an intrinsic scatter of 0.2 added in the latter case). The best-fitting slopes of the latter two (Y|X) relations are in excellent agreement with those reported by the main three reference studies. We stress that we find *no* significant correlation between Γ_{simple} and

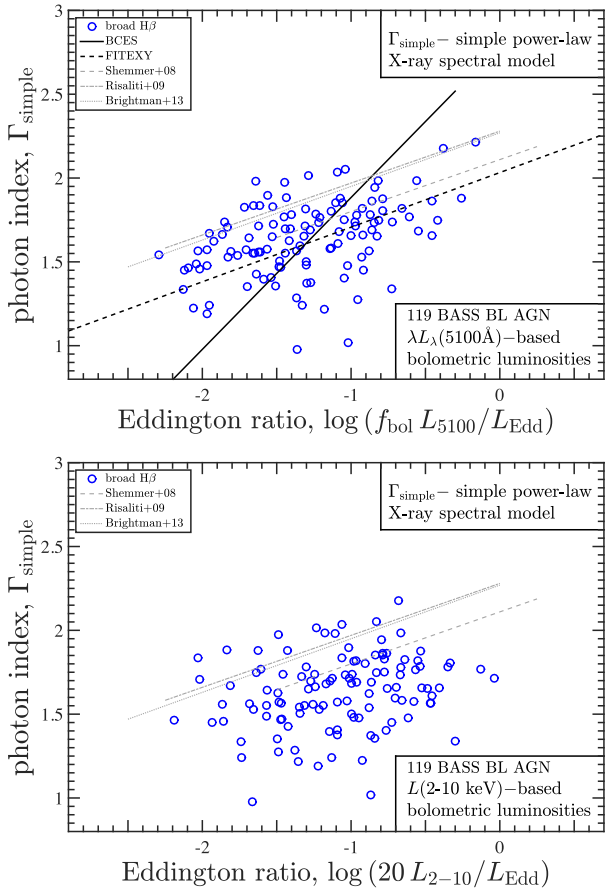

Figure 8. An attempt to compare BASS with previous studies of the Γ_x–L/L_{Edd} relation in broad-line, $z \gtrsim 1$ AGN. Here, the photon index Γ_{simple} is derived from a simplified spectral model of a power law, fit to the softer X-ray data of a subset of 119 unobscured ($\log(N_H/cm^{-2}) \leq 22$), broad-line AGN where M_{BH} is determined from broad Hβ. *Top*: L/L_{Edd} is estimated from L_{5100}. These data exhibit a statistically significant correlation, unlike what we found when considering Γ_{tot} (cf. the bottom-right panel of Fig. 6). *Bottom*: L/L_{Edd} is estimated from L_{2-10}. No correlation is found in this case.

the primary, L_{2-10}-based estimates of L/L_{Edd} ($P = 0.8$ per cent), as seen in the bottom panel of Fig. 8. This is an important point, as some of the studies that reported strong Γ_x–L/L_{Edd} correlations (e.g. R09, B13) relied, at least partially, on L_{2-10}-based determinations of L/L_{Edd}, and not on purely L_{5100}-based ones.

Thus, it appears that the photon index derived from a simplified X-ray spectral model of a power-law traces a Γ_x–L/L_{Edd} correlation that is very similar to what was reported in previous studies. However, such a correlation is *not* seen when using more elaborate X-ray spectral models, nor when using X-ray-based determinations of L/L_{Edd}. We conclude that the tension between our overall result for the BASS AGN – of no strong Γ_x–L/L_{Edd} relation for broad-line AGN – and that of previous studies, might be indeed driven by the limited spectral coverage, or the simplified spectral model used in some of the reference studies.

4.3 Using Γ_x as a BH growth indicator

As first pointed out by Shemmer et al. (2008), one of the exciting implications of a strong and tight relation between Γ_x and L/L_{Edd} is the possibility to use large X-ray surveys to construct nearly complete distributions of L/L_{Edd}, particularly for high-redshift sources

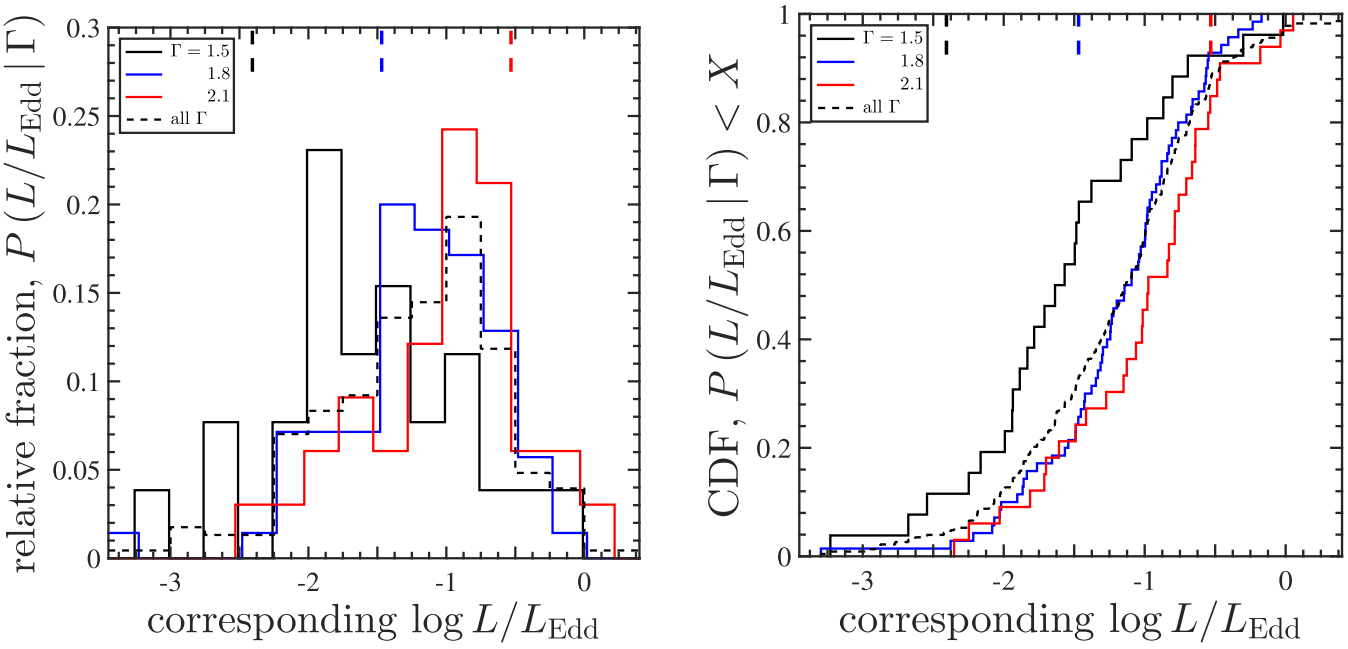

Figure 9. Testing the usability of Γ_x as a predictor of L/L_{Edd}. *Left*: the *observed* distribution of L/L_{Edd} for the 228 BASS sources in our sample, split into three non-overlapping bins of Γ_{tot}: $\Gamma_{tot} = 1.6$, 1.8, and 2.1 (all bins have widths ± 0.1; solid lines). The dashed histogram traces the distribution of L/L_{Edd} among the entire sample of 228 BASS sources. The short vertical dashed lines near the top mark the L/L_{Edd} predicted from the Γ_x–L/L_{Edd} relation reported in Brightman et al. (2013). *Right*: same distributions of L/L_{Edd}, but represented as cumulative fractions. Both panels demonstrate the significant scatter in L/L_{Edd} at nearly fixed Γ_x; the significant overlap between the range of L/L_{Edd} covered by each sub-sample; and the differences between the distributions' peaks (or medians) and the 'predicted' values.

in deep extragalactic fields, where this key quantity is otherwise hard to measure (e.g. Trakhtenbrot & Netzer 2012; Trakhtenbrot et al. 2016). The study of Brightman et al. (2013) can be considered as a demonstration of such an approach within a dedicated survey (COSMOS). Moreover, the recent study of Brightman et al. (2016) suggested that this approach may also be applicable to heavily obscured (CT) AGN, potentially providing a unique probe of the accretion rates among these elusive objects.

However, our sample and analysis highlight the limitations associated with using Γ_x measurements to predict L/L_{Edd}. We first recall that the overall scatter in the Γ_x–L/L_{Edd} plane is large ($\sim$0.3 dex; see Figs 2–6), and that the few statistically significant relations we find between Γ_x and L/L_{Edd} are weak (i.e. have flat slopes, $\alpha \simeq 0.15$).

To further assess the usability of Γ_x as a predictor of L/L_{Edd}, we show in Fig. 9 the distributions of L/L_{Edd} among three subsets of BASS sources with (almost) fixed Γ_x values, $\Gamma_x = 1.5$, 1.8, and 2.1, with the Γ_x bins defined within ± 0.1 of these values. Here, we used Γ_{tot} and the L_{2-10}-based estimates of L/L_{Edd}, for the sample of 228 BASS sources at $0.01 < z < 0.5$ with high-quality X-ray data ($N_{counts} > 1000$) – the same measurements as those presented in Fig. 3. For all three Γ_x bins, the corresponding distributions of L/L_{Edd} span about two orders of magnitude, covering the entire range $L/L_{Edd} \sim 0.01$–1. This range is comparable to what is observed for other large samples of luminous AGN, at least out to $z \sim 2$ (e.g. Trakhtenbrot & Netzer 2012; Kelly & Shen 2013; Schulze et al. 2015, and references therein). For the $\Gamma_x = 1.8 \pm 0.1$ bin alone,[8] the 1σ interquartile range in L/L_{Edd} (i.e. corresponding to the 16–84 per cent quantile range) covers roughly 1.1 dex. This is qualitatively similar to the behaviour of the overall distribution of L/L_{Edd} in our sample (i.e. regardless of Γ_x; dashed lines in Fig. 9). Moreover, the ranges in L/L_{Edd} for the three Γ_x subsets show considerable overlap, and in particular the distributions of L/L_{Edd} corresponding to the $\Gamma_x = 1.8$ bin is similar to that of the $\Gamma_x = 2.1$ bin (a two-sided Kolmogorov–Smirnov test resulted in $P_{K\text{-}S} = 16.9$ per cent). Finally, these distributions of L/L_{Edd} do *not* agree with the predictions of the Γ_x–L/L_{Edd} relations, as demonstrated by the short vertical (dashed) lines plotted near the top of both panels in Fig. 9, which mark the L/L_{Edd} values predicted from the B13 Γ_x–L/L_{Edd} relation, for each of our Γ_x bins.

The limitations on measuring L/L_{Edd} from Γ_x are further demonstrated by the corresponding correlation analysis. The best-fitting BCES relation we find for our primary sample (i.e. 228 sources) is

$$L/L_{Edd} = (0.71 \pm 0.27)\,\Gamma_{tot} - (2.44 \pm 0.48), \quad (3)$$

which is consistent, within the considerable uncertainties, to the relation reported by S08 (their eq. 2). The uncertainties on the best-fitting parameters in eq. (3) are so large that for a given Γ_{tot} with zero measurement uncertainty, they predict values of L/L_{Edd} with a 1σ interpercentile range of 1.37 dex (i.e. the 16–84 per cent percentile range). Moreover, the corresponding FITEXY (L/L_{Edd} – Γ_{tot}) analysis suggests that a satisfactory fit, with $\chi^2/\nu \simeq 1$, can only be obtained with the addition of a significant level of intrinsic scatter, exceeding 0.6.

Notwithstanding these limitations, it might still be possible to identify subsets of extremely high- or low-L/L_{Edd} AGN, probed by correspondingly extreme Γ_x (i.e. $\Gamma_x \gtrsim 2.3$ or $\lesssim 1.2$). This is supported by the relatively clear separation between the peaks (and medians) of the distributions seen for $\Gamma_x = 1.5$ and 2.1 in Fig. 9. We note, however, that such extreme Γ_x are only observed among

[8] Corresponding to the median value of Γ_{tot} for our primary sample (see Fig. 1).

a minority of AGN, out to $z \sim 4$ (e.g. Just et al. 2007; Brandt & Alexander 2015; Cappelluti et al. 2016; Marchesi et al. 2016).

We conclude that the large scatter and weak correlations (at best) in the Γ_x–L/L_{Edd} plane significantly hinder the prospects of using Γ_x measurements to establish the distribution of L/L_{Edd} among samples of high-redshift AGN.

4.4 Possible physical links between Γ_x and L/L_{Edd}

Previous studies have tried to explain the positive Γ_x–L/L_{Edd} correlation through a picture where the increasing L/L_{Edd} is causing an increased UV radiation, which in turn causes more efficient cooling in the corona. In principle, one may expect a similar trend of increasing Γ_x with *decreasing* M_{BH}, as in the framework of geometrically thin, radiatively thick accretion discs this is also expected to increase the UV incident radiation (e.g. Davis & Hubeny 2006; Done et al. 2012; Davis & Laor 2011).

We however recall that our analysis showed no correlation between Γ_x and M_{BH} (Fig. 7). One way to accommodate this lack of trend with the aforementioned physical picture is if the X-ray-emitting corona is located closer to the disc for lower M_{BH} systems, therefore *reducing* the amount of incident UV radiation. Such trends are indeed suggested by some reverberation mapping studies (see e.g. De Marco et al. 2013; Kara et al. 2013, and the review by Uttley et al. 2014).

We conclude that any scenario that connects the observed Γ_x–L/L_{Edd} relation to variations in the UV radiation field that is upscattered by the hot, X-ray emitting corona, should also account for the lack of observed relation between Γ_x and M_{BH} (and for that matter, with L_X; see again Fig. 7).

5 CONCLUSIONS

We presented a detailed analysis of the links between the hard X-ray photon index, Γ_x, and the (normalized) accretion rate, L/L_{Edd}, for a large sample of hard X-ray-selected, low-redshift AGN, as part of the BASS project. Our analysis was motivated by several earlier studies that identified significant, positive correlations between Γ_x and L/L_{Edd}, over a broad range of redshifts. The low-redshift BASS sample allowed us to study these relations over a wide range of L_{AGN}, M_{BH}, and L/L_{Edd}. The high-quality and broad spectral coverage of the BASS data – unprecedented among studies that address the Γ_x–L/L_{Edd} relation – allowed us to examine, for the first time in this context, the role of alternative determinations of the key quantities, and of the different methods used to derive them. Our main conclusions are as follows:

(i) Despite a significant amount of scatter, we find a weak (but statistically significant) correlation between Γ_x and L/L_{Edd} among our primary sample of 228 AGN. This correlation is robust to the choice of Γ_x.

(ii) The best-fitting Γ_x–L/L_{Edd} relations we obtain have flatter slopes than those reported by previous studies. Moreover, these best-fitting relations fail to reduce the scatter in the Γ_x–L/L_{Edd} plane.

(iii) We find either no, or weak evidence for a Γ_x–L/L_{Edd} correlation when considering, separately, the subsets of AGN that differ in the method used to derive M_{BH} (and therefore, L/L_{Edd}). In particular, we find no correlation for the subset of AGN with the most reliable, 'direct' mass estimates.

(iv) We find no statistically significant correlations between Γ_x and either the L/L_{Edd} estimates based on L_{BAT}, nor with L_{2-10}, M_{BH}, or the width of the broad Balmer emission lines.

(v) A Γ_x–L/L_{Edd} correlation that is consistent with those reported in previous studies *does* emerge, for a subset of broad-line AGN, when adopting a simplified, power law only spectral model fit to the lower energy X-ray data, and only when coupled with L/L_{Edd} determinations that are based on the *optical* continuum emission.

(vi) We caution that the prospects of using the Γ_x–L/L_{Edd} relation for deriving distributions of L/L_{Edd} (and indeed M_{BH}) from deep X-ray surveys are limited due to the large scatter in the Γ_x–L/L_{Edd} plane, the weakness of the correlations we find, and their dependence on specific methodological choices (i.e. bolometric corrections and X-ray energy ranges).

Our analysis clearly demonstrates the complexity of the Γ_x–L/L_{Edd} plane, even for a uniformly selected sample of nearby AGN, with a rich collection of multiwavelength data, and a careful, elaborate spectral analysis. It appears that the previously reported strong relations between Γ_x and L/L_{Edd} may be, at least partially, driven by methodological choices (i.e. L_{bol} prescriptions) and/or limited spectral coverage and modelling in the X-ray regime. Our results hint that an underlying physical mechanism that links the shape of the X-ray SED with L/L_{Edd} may indeed be at work, but is not yet well understood.

The existence and robustness of the Γ_x–L/L_{Edd} relation may be re-evaluated with yet larger, unbiased samples of hard X-ray-selected AGN, provided by ongoing surveys using the *Swift* and *NuSTAR* missions. In particular, the *NuSTAR* mission is providing high sensitivity and high spatial resolution hard X-ray data for hundreds of AGN (Civano et al. 2015; Lansbury et al. 2017), reaching lower luminosities and/or higher redshifts than previous hard X-ray studies.

ACKNOWLEDGEMENTS

We thank the anonymous referee, as well as M. Brightman, O. Shemmer, and R. Bär for their constructive comments, which helped us to improve the manuscript. This work made use of the MATLAB package for astronomy and astrophysics (Ofek 2014). This research has made use of the NED, which is operated by the Jet Propulsion Laboratory, California Institute of Technology, under contract with the National Aeronautics and Space Administration. This research has made use of NASA's Astrophysics Data System.

CR acknowledges financial support from the China-CONICYT fund, FONDECYT 1141218 and Basal-CATA PFB-06/2007. MK acknowledges support from the Swiss National Science Foundation (SNSF) through the Ambizione fellowship grant PZ00P2_154799/1, and from NASA through ADAP award NNH16CT03C. KS and KO acknowledge support from the Swiss National Science Foundation (SNSF) through grants 200021_157021, PP00P2_138979, and PP00P2_166159. ET acknowledges support from CONICYT-Chile grants Basal-CATA PFB-06/2007 and FONDECYT Regular 1160999. The work of DS was carried out at the Jet Propulsion Laboratory, California Institute of Technology, under a contract with NASA. MB acknowledges support from NASA Headquarters under the NASA Earth and Space Science Fellowship Program, grant NNX14AQ07H.

REFERENCES

Akritas M. G., Bershady M. A., 1996, ApJ, 470, 706
Baumgartner W. H., Tueller J., Markwardt C. B., Skinner G., Barthelmy S., Mushotzky R. F., Evans P. A., Gehrels N., 2013, ApJS, 207, 19
Berney S. et al., 2015, MNRAS, 454, 3622
Bian W., 2005, Chin. J. Astron. Astrophys., 5, 289
Bianchi S., Guainazzi M., Matt G., Fonseca Bonilla N., 2007, A&A, 467, L19

Brandt W. N., Alexander D. M., 2015, A&AR, 23, 1
Brandt W. N., Boller T., 1998, Astron. Nachr., 319, 163
Brandt W. N., Mathur S., Elvis M., 1997, MNRAS, 285, L25
Brightman M. et al., 2013, MNRAS, 433, 2485 (B13)
Brightman M. et al., 2016, ApJ, 826, 93
Cappelluti N. et al., 2016, ApJ, 823, 95
Cappi M., Mihara T., Matsuoka M., Brinkmann W., Prieto M. A., Palumbo G. G. C., 1996, ApJ, 456, 141
Civano F. et al., 2015, ApJ, 808, 185
Constantin A., Green P. J., Aldcroft T., Kim D.-W., Haggard D., Barkhouse W., Anderson S. F., 2009, ApJ, 705, 1336
Davis S. W., Hubeny I., 2006, ApJS, 164, 530
Davis S. W., Laor A., 2011, ApJ, 728, 98
De Marco B., Ponti G., Cappi M., Dadina M., Uttley P., Cackett E. M., Fabian A. C., Miniutti G., 2013, MNRAS, 431, 2441
Done C., Davis S. W., Jin C., Blaes O., Ward M., 2012, MNRAS, 420, 1848
Elvis M. et al., 1994, ApJS, 95, 1
Fabian A. C., Vasudevan R. V., Gandhi P., 2008, MNRAS, 385, L43
Fabian A. C., Vasudevan R. V., Mushotzky R. F., Winter L. M., Reynolds C. S., 2009, MNRAS, 394, L89
Fanali R., Caccianiga A., Severgnini P., Della Ceca R., Marchese E., Carrera F. J., Corral A., Mateos S., 2013, MNRAS, 433, 648
Gehrels N. et al., 2004, ApJ, 611, 1005
Greene J. E., Ho L. C., 2005, ApJ, 630, 122
Grier C. J. et al., 2013, ApJ, 773, 90
Grupe D., Komossa S., Leighly K. M., Page K. L., 2010, ApJS, 187, 64
Gültekin K., Cackett E. M., Miller J. M., Di Matteo T., Markoff S., Richstone D. O., 2012, ApJ, 749, 129
Ho L. C., Kim M., 2016, ApJ, 821, 48
Iwasawa K., Taniguchi Y., 1993, ApJL, 413, L15
Jin C., Ward M., Done C., 2012, MNRAS, 425, 907
Just D. W., Brandt W. N., Shemmer O., Steffen A. T., Schneider D. P., Chartas G., Garmire G. P., 2007, ApJ, 665, 1004
Kamizasa N., Terashima Y., Awaki H., 2012, ApJ, 751, 39
Kara E., Fabian A. C., Cackett E. M., Uttley P., Wilkins D. R., Zoghbi A., 2013, MNRAS, 434, 1129
Kawamuro T., Ueda Y., Tazaki F., Ricci C., Terashima Y., 2016a, ApJS, 225, 14
Kawamuro T., Ueda Y., Tazaki F., Terashima Y., Mushotzky R., 2016b, ApJ, 831, 1
Kelly B. C., Shen Y., 2013, ApJ, 764, 45
Kormendy J., Ho L. C., 2013, ARA&A, 51, 511
Lamperti I. et al., 2017, MNRAS, 467, 540
Lansbury G. B. et al., 2017, ApJ, 836, 99
Lusso E. et al., 2010, A&A, 512, A34
Magdziarz P., Blaes O. M., Zdziarski A. A., Johnson W. N., Smith D. A., 1998, MNRAS, 301, 179
Marchesi S. et al., 2016, ApJ, 817, 34
Marconi A., Risaliti G., Gilli R., Hunt L. K., Maiolino R., Salvati M., 2004, MNRAS, 351, 169
Mejía-Restrepo J. E., Trakhtenbrot B., Lira P., Netzer H., Capellupo D. M., 2016, MNRAS, 460, 187
Netzer H., 2013, The Physics and Evolution of Active Galactic Nuclei. Cambridge Univ. Press, Cambridge
Ofek E. O., 2014, Astrophysics Source Code Library, record ascl:1407.005
Oh K., Yi S. K., Schawinski K., Koss M., Trakhtenbrot B., Soto K. T., 2015, ApJS, 219, 1
Oh K. et al., 2017, MNRAS, 464, 1466
Park D. et al., 2012, ApJ, 747, 30
Peterson B. M., 2014, SSRv, 183, 253
Porquet D., Reeves J. N., O'Brien P., Brinkmann W., 2004, A&A, 422, 85
Pounds K., Done C., Osborne J. P., 1995, MNRAS, 277, L5
Ricci C., Paltani S., Ueda Y., Awaki H., 2013, MNRAS, 435, 1840
Ricci C., Ueda Y., Koss M. J., Trakhtenbrot B., Bauer F. E., Gandhi P., 2015, ApJL, 815, L13
Risaliti G., Young M., Elvis M., 2009, ApJL, 700, L6 (R09)
Schulze A. et al., 2015, MNRAS, 447, 2085
Shemmer O., Brandt W. N., Netzer H., Maiolino R., Kaspi S., 2006, ApJL, 646, L29
Shemmer O., Brandt W. N., Netzer H., Maiolino R., Kaspi S., 2008, ApJ, 682, 81 (S08)
Shen Y., 2013, Bull. Astron. Soc. India, 41, 61
Shen Y., Liu X., 2012, ApJ, 753, 125
Sobolewska M. A., Papadakis I. E., 2009, MNRAS, 399, 1597
Trakhtenbrot B., Netzer H., 2012, MNRAS, 427, 3081
Trakhtenbrot B. et al., 2016, ApJ, 825, 4
Tremaine S. et al., 2002, ApJ, 574, 740
Uttley P., Cackett E. M., Fabian A. C., Kara E., Wilkins D. R., 2014, A&AR, 22, 72
Vasudevan R. V., Fabian A. C., 2007, MNRAS, 381, 1235
Vasudevan R. V., Mushotzky R. F., Winter L. M., Fabian A. C., 2009, MNRAS, 399, 1553
Vasudevan R. V., Mushotzky R. F., Gandhi P., 2013, ApJL, 770, L37
Wang J.-M., Watarai K.-Y., Mineshige S., 2004, ApJL, 607, L107
Winter L. M., Mushotzky R. F., Reynolds C. S., Tueller J., 2009a, ApJ, 690, 1322
Winter L. M., Mushotzky R. F., Terashima Y., Ueda Y., 2009b, ApJ, 701, 1644
Winter L. M., Veilleux S., McKernan B., Kallman T. R., 2012, ApJ, 745, 107
Woo J.-H., Schulze A., Park D., Kang W.-R., Kim S. C., Riechers D. A., 2013, ApJ, 772, 49
Yang Q. X., Xie F. G., Yuan F., Zdziarski A. A., Gierliński M., Ho L. C., Yu Z., 2015, MNRAS, 447, 1692
Younes G., Porquet D., Sabra B., Reeves J. N., 2011, A&A, 530, A149
Young M., Elvis M., Risaliti G., 2009, ApJS, 183, 17
Zdziarski A. A., Lubi P., Gilfanov M., Revnivtsev M., 2003, MNRAS, 342, 355

APPENDIX A: RESULTS OF ADDITIONAL CORRELATION ANALYSIS

As noted in Section 3.3, we have performed a series of correlation tests for different subsets of AGN in order to verify that our main results are not driven by the particular choices made through the sample definition and spectral analysis parts of our work. Table A1 presents the results of the correlation hypothesis tests for these subsets, which include:

(i) *AGN at 0.05 < z < 0.5* – a subset where the effects of spectroscopic aperture (relevant for M_{BH}, and there L/L_{Edd}, determination) are minimal. For this sample, we find no statistically significant correlation, neither when considering all M_{BH} subsets (84 sources), nor when considering each of these subsets separately (see *P*-values in Table A1).

(ii) *AGN with SDSS-based optical spectroscopy* – a subset where the (relative and absolute) flux calibration is optimal, and where aperture effects are small and well understood. For this sample of 47 sources, we find a result similar to the general one: only the entire sample results in a significant correlation, while the relevant main M_{BH} subset (i.e. single-epoch estimates based on SDSS spectra) does not show a correlation.

(iii) *AGN with 0.01 < L/L_{Edd} < 1* – a subset dominated by broad-line sources, which could in principle capture an underlying, positive Γ_x–L/L_{Edd} correlation even if this relation flattens (or becomes an anticorrelation) at very low or very high L/L_{Edd}. For this sample of 195 sources (mostly broad-line AGN), we find a result similar to the general one: the entire sample results in a statistically significant, but weak correlation; the three M_{BH} subsets (within the $L/L_{Edd} > 0.01$ sample) do not show a correlation.

Table A1. BASS Γ_x–L/L_{Edd} correlations: significance tests for minor subsets. Statistically significant *P*-values are highlighted in bold.

L_{bol} tracer	Γ	Sub-sample	N	P-value (per cent)	r_s
$C \cdot L_{2-10}$	Γ_{tot}	$0.05 < z < 0.5$ – all	84	8.1	–
		– direct M_{BH}	9	61.3	–
		– single-epoch M_{BH}	64	9.9	–
		– σ_*-based M_{BH}	11	32.7	–
$C \cdot L_{2-10}$	Γ_{tot}	SDSS spectra – all	47	1.70	–
		– single-epoch M_{BH}	33	54.7	–
		– σ_*-based M_{BH}	14	10.4	–
$C \cdot L_{2-10}$	Γ_{tot}	$0.01 < L/L_{Edd} < 1$ – all	195	$\mathbf{4.1 \times 10^{-2}}$	0.251
		– direct M_{BH}	29	63.2	–
		– single-epoch M_{BH}	140	0.83	–
		– σ_*-based M_{BH}	26	18.7	–
$C \cdot L_{2-10}$	Γ_{tot}	$\log N_H < 23$ – all	188	$\mathbf{1.7 \times 10^{-3}}$	0.308
		– direct M_{BH}	26	65.5	–
		– single-epoch M_{BH}	137	0.25	–
		– σ_*-based M_{BH}	25	39.5	–
$C \cdot L_{2-10}$	$\Gamma_{0.3-10}$	$\log N_H < 23$ – all	188	$\mathbf{1.6 \times 10^{-5}}$	0.371
		– direct M_{BH}	26	91.4	–
		– single-epoch M_{BH}	137	**0.067**	0.287
		– σ_*-based M_{BH}	25	39.5	–
$C \cdot L_{2-10}$	Γ_{nEc}	$\log N_H < 23$ – all	188	$\mathbf{5.3 \times 10^{-6}}$	0.384
		– direct M_{BH}	26	93.8	–
		– single-epoch M_{BH}	137	**0.0058**	0.337
		– σ_*-based M_{BH}	25	88.0	–
$C \cdot L_{2-10}$	Γ_{tot}	No warm absorbers – all	184	$\mathbf{3.4 \times 10^{-3}}$	0.301
		– direct M_{BH}	20	69.1	–
		– single-epoch M_{BH}	115	0.65	–
		– σ_*-based M_{BH}	49	39.2	–

(iv) *AGN with log* $(N_H/cm^{-2}) < 23$ – a subset where the effects of Compton scattering on the X-ray spectral decomposition are minimal.

For this sample of 188 sources we find, again, a result similar to the general one: only the entire sample results in a significant correlation, while the two main M_{BH} subsets (within the $\log(N_H/cm^{-2}) < 23$ sample) do not show a correlation. For this subset, we also tested correlations involving $\Gamma_{0.3-10}$ and Γ_{nEc}, which are expected to be most sensitive to a Compton scattering component. Indeed, we find that for this subset the correlations involving $\Gamma_{0.3-10}$ and Γ_{nEc} are somewhat stronger that those found with Γ_{tot}. However, the qualitative outcome remains identical.

(v) *AGN without warm absorbers* – the presence of significant ionized absorption in the X-ray spectrum might lead to deviation of Γ_x from the intrinsic value. For this sample of 184 sources, we again find a result consistent with the general one: the entire sample results in a significant correlation, while the two main M_{BH} subsets do not show a correlation.

This paper has been typeset from a TEX/LATEX file prepared by the author.